Earth-Science Reviews 109 (2011) 94–112

Contents lists available at SciVerse ScienceDirect

Earth-Science Reviews

journal homepage: www.elsevier.com/locate/earscirev

On the origin of Cenozoic and Mesozoic "third-order" eustatic sequences

Slah Boulila [a,b,*], Bruno Galbrun [a], Kenneth G. Miller [c], Stephen F. Pekar [d], James V. Browning [c], Jacques Laskar [b], James D. Wright [c]

[a] CNRS - UMR 7193 ISTeP 'Institut des Sciences de la Terre-Paris', Université Paris VI, case 117, 4 place Jussieu, 75252 Paris cedex 05, France
[b] ASD, IMCCE-CNRS UMR8028, Observatoire de Paris, UPMC, 77, Avenue Denfert-Rochereau, 75014 Paris, France
[c] Department of Earth and Planetary Sciences, Rutgers University, Piscataway, New Jersey 08854, USA
[d] School of Earth and Environmental Sciences, Queens College, 65–30 Kissena Blvd, Flushing, NY 11367, USA

ARTICLE INFO

Article history:
Received 27 May 2010
Accepted 22 September 2011
Available online 1 October 2011

Keywords:
third-order eustatic sequences
~1.2- and ~2.4-myr astronomical cycles
Cenozoic
Mesozoic
eustatic sequence hierarchy

ABSTRACT

The origin of third-order eustatic sequences is reviewed by comparing recent sequence stratigraphic data to the latest, best-constrained astronomical model. Middle Eocene to Holocene icehouse sequences correspond to ~1.2 myr obliquity cycles. Constraints from oxygen isotope records highlight the link between "icehouse" sea-level lowerings, sequence boundaries, and ~1.2 myr obliquity nodes. Mesozoic greenhouse sequences show some relation with the ~2.4 myr eccentricity cycles, suggesting that orbital forcing contribute to sea-level change.

We suggest that during the icehouse, large ice sheets associated with significant glacioeustatic changes (>>25 m up to 120 m changes) were mainly governed by obliquity forcing. During icehouse worlds, obliquity forcing was the stongest control on global sea-level and depositional sequences. Additionally, during the Middle Eocene, third-order sequences were glacioeustatically driven in tune with ~1.2 myr obliquity cycle, suggesting that the presence of significant ice sheets is earlier than previously supposed (i.e., Early Eocene). In contrast, during greenhouse worlds (e.g., ephemeral, small to medium sized or no ice sheets; 0- ~25 m glacioeustatic changes), the expression of obliquity in the sedimentary record is weak and intermittent. Instead, the eccentricity signature, which is the modulator of climatic precession, is documented. Moreover, we presume that greenhouse sequences on the myr scale are global and hence cannot be caused by regional tectonism (e.g., intraplate stress or mantle "hot blobs"). Instead, the eccentricity link implies a weaker glacioeustatic control because thermoeustasy is too small to explain the sea-level changes.

Stratigraphically well-documented fourth-order sequences may be linked to the astronomically stable (strongest amplitude) 405-kyr eccentricity cycle and possibly to ~160-200-kyr obliquity modulation cycles, fifth-order sequences to the short (~100-kyr) eccentricity cycles, and finally sixth-order sequences to the fundamental obliquity (~40 kyr) and climatic precession (~20 kyr) cycles. These astronomical cycles could be preserved in the sedimentary record, and have been demonstrated to control sea-level changes. Accordingly, by placing depositional sequence orders into a high-resolution temporal framework (i.e., orbital periodicities), standardization of eustatic sequence hierarchy may be possible.

Contents

* Corresponding author at: CNRS - UMR 7193 ISTeP 'Institut des Sciences de la Terre-Paris', Université Paris VI, case 117, 4 place Jussieu, 75252 Paris cedex 05, France. Tel.: +33 144274163; fax: +33 144273831.

E-mail addresses: slah.boulila@upmc.fr (S. Boulila), bruno.galbrun@upmc.fr (B. Galbrun), kgm@rci.rutgers.edu (K.G. Miller), stephen.pekar@dc.cuny.edu (S.F. Pekar), jvb@rci.rutgers.edu (J.V. Browning), Jacques.Laskar@imcce.fr (J. Laskar), jdwright@rci.rutgers.edu (J.D. Wright).

0012-8252/$ – see front matter © 2011 Elsevier B.V. All rights reserved.
doi:10.1016/j.earscirev.2011.09.003

1. Introduction

Global sea-level (eustatic) change is one of the major controls on the sedimentary record (e.g., Sloss, 1963; Vail et al., 1977; Kominz et al., 1998; Miller et al., 2005a). The definition of depositional sequences by Exxon Production Research Company (Vail et al., 1977; Haq et al., 1987), and their interpretation of a sea-level control on deposition, led to debates regarding timing, amplitudes, and mechanism of these eustatic changes that continue today (e.g., Christie-Blick et al., 1990; Miller and Mountain, 1996; Pekar and Miller, 1996; Miller et al., 1998; Kominz and Pekar, 2001; Pekar et al., 2001, 2002; Müller et al., 2008; and many others). Vail et al. (1977) divided these depositional sequences temporally into six orders ranging from tens of millions years (first- and second-order) to a few tens of thousands years (sixth order). One of the outstanding questions of the past 30 years is the origin of third-order eustatic sequences (0.5-3 myr durations, Haq et al., 1987; Vail et al., 1991) in Cenozoic and Mesozoic strata (e.g., Lourens and Hilgen, 1997; Grant et al., 1999; Strasser et al., 2000; Gale et al., 2002, 2008; Matthews and Frohlich, 2002; Boulila et al., 2008a, 2010b). The definition of the third-order sequence at spatial and temporal scales has been hampered by several constraints such as the potential of (sediment) preservation, which depends on depositional environments and settings, the lack or absence of chronostratigraphic control, and difficulties in deciphering sequence orders. For example, a spatially patchy distribution of sequences on a given depositional profile is related to variations in accommodation space, which depends in turn on sediment migration and supply, and differential subsidence (e.g., Christie-Blick et al., 1990). In contrast, variable durations of third-order sequences (0.5 to 3 myr) could be related to difficulties in deciphering sequence hierarchy, uncertainties in age models used to date sequence boundaries, possible undetected hiatuses, and/or pseudo-periodic variations of the forcing process itself (Section 2, and Tables 1 and 3).

The amplitude of eustatic oscillation is a critical criterion for sequence order determination (e.g., Vail et al., 1977). Whereas studies have generally shown that the number and age of cycle chart sea-level falls (Vail et al., 1977; Haq et al., 1987) is generally correct, the amplitude and shape of their curve is not correct, with amplitudes typically overestimates by 2–2.5 times (Miller and Mountain, 1996, Miller et al., 2005a). Even the relative difference between sea level events in the cycle chart may not be correct, calling into question their use in identifying sea-level hierarchy (Miller et al., 2011). Likewise, geophysical logging proxies in sections with low sedimentation rates could lead to different sequence stratigraphic interpretation compared to sections with high sedimentation rates (e.g., Jacquin et al., 1998 discussed in Boulila et al., 2010b). These significant problems, related to duration and amplitude of eustatic change, make it difficult to identify third-order depositional sequences.

New developments in sequence stratigraphic modelling provide improved quantitative estimates of amplitudes of global sea-level change (e.g., Kominz and Pekar, 2001). Glacioeustatic fluctuations cause global seawater $\delta^{18}O$ changes, which are recorded by benthic

Table 1
Compiled Oligocene-Miocene sequence stratigraphy of the New Jersey, oxygen isotope data (references below), and La2004 ~1.2-myr obliquity nodes (Laskar et al., 2004). New Jersey sequence stratigraphy are from Miller et al. (1998), and updated from Kominz et al. (2008), otherwise sources are shown in superscript letters, from left to right, as follows. First column, V: De Verteuil (1997), Second column, S: Sugarman et al. (2005). Oxygen isotope data are from Miller et al. (1991, 1998), otherwise sources are shown in superscript letters, from left to right, as follows. Third column: Oi2d is a possible additional event according to Pälike et al. (2006a), Oi2x corresponds to the unnamed event in Miller et al. (1998). Fourth column: T: Turco et al. (2002), Lir: Lirer et al. (2009), L: Lourens and Hilgen (1997), Wes: Westerhold et al. (2005), B: Billups et al. (2002), P: Pekar and DeConto (2006). R: Miller et al.'s new revisions (unpublished). * Oligocene timescale is based on the ATS model of Pälike et al. (2006a). Miocene timescale is rescaled to GTS2004 (Gradstein et al., 2004). NR : not recognized. Oxygen isotope events were attributed to sequence boundaries (i.e., sea-level falls) (e.g., Miller and Mountain, 1996; Miller et al., 1998).

3rd order sequence	Basal sequence boundary/Hiatus age (Ma)	d18O event	d18O maximum age (Ma)	La2004 obliquity node age (Ma)
Kw-Ch6V	8.23-8.04S	NR		7.94
Kw-Ch5V	8.87-8.66S	Mi7	8.7	8.98
Kw-Ch4V	9.75-9.49S	Mi6	10.3(10.4T)	10.34
Kw-Ch3V	11.58-10.37	Mi5	11.7(11.4T,11.42Lir)	11.40
Kw-Ch2V	12.75-12.53	Mi4	12.9(12.8L,13.2Wes)	12.77
Kw-Ch1	12.94	Mi3	13.7	13.65
Kw3	15.58-14.67	Mi2a	14.8	14.99
Kw2c	16.48-16.06	Mi2	16.1(16.1B, 16.2R)	16.04
Kw2b	18.07-17.58	Mi1b	17.7 (17.8B,17.6P, 17.5R)	17.40
Kw2a	19.15-19.06	Mi1ab	18.2 (18.2P, 18.7R)	18.28
Kw1c	19.78	Mi1aa	19.7 (19.9P, 19.8R)	19.67
Kw1b	20.99-20.61	Mi1a	20.8 (21.0B,20.6P, 21.15R)	20.72
Kw1a	21.99-21.2	unnamed	22.0R	21.92
Kw0	23-22.82	Mi1	23.0 (23.1R)	22.98
O7	24.3	Oi2d	24.3	24.33
O6	25.5-25.7	Oi2c	25.1	25.39
O5	26.9-27.1	Oi2b	26.4	26.76
O4	27.9-28.3	Oi2a	27.9	27.64
O3	28.9	Oi2x	28.8	28.98
O2b	30.1-29.5	Oi2	30.0	30.06
O2	31.6-32.1	Oi1b	31.8	31.58
O1	32.9-33.1	Oi1a	32.9	32.64
ML	33.8-33.5	Oi1	33.65	33.99

and planktonic foraminifera, although these global changes can be overprinted by temperature. Conjointly used benthic foraminiferal Mg/Ca ratios and $\delta^{18}O$ provide a means to trace the evolution of ice sheets and the associated sea-level changes (e.g., Billups and Schrag, 2002). Interestingly, when used together, sedimentology and isotopic stratigraphy could constrain the amplitudes of sea-level change (e.g., Pekar et al., 2002; John et al., 2004, 2011). Durations of sequences could be constrained if the forcing processes are known. Particularly, Earth's orbital parameters (climatic precession, obliquity, and eccentricity) represent one of the main external driving forces on climate and sea-level changes via insolation intensity (e.g., Hays et al., 1976; Imbrie et al., 1984; Strasser et al., 2006; Naish et al., 2009; and many others). Variations of these parameters have been calculated with precision for the last 50 million years (Laskar et al., 2004, 2011).

Numerous studies of high-resolution $\delta^{18}O$ records have demonstrated that climate variations are consistent with the quasi-periodic orbital parameters: climatic precession, obliquity and eccentricity, during the later Cenozoic icehouse (younger than 33.8 Ma). Particularly, 41 kyr obliquity forcing appears to be the primary driver of glacial variability in this icehouse world (e.g., Zachos et al., 2001a; Holbourn et al., 2007). More interestingly, the ~1.2-myr obliquity cycle was demonstrated as a beat in the major glacial episodes (Zachos et al., 2001b; Wade and Pälike, 2004; Pälike et al., 2006a,b). On the other hand, theoretical modelling of the greenhouse sequences shows that glacioeustasy may have been controlled by eccentricity. Particularly, Matthews and Frohlich (2002) showed that glacioeustatic changes appear in the 405-kyr and ~2.4-myr eccentricity bands during Cretaceous and Jurassic intervals. Matthews and colleagues generalized their eccentricity-forcing model for the Cenozoic and Mesozoic eras, i.e., icehouse and greenhouse periods (e.g., Mattews and Al-Husseini, 2010). Even if Matthews and colleagues did not consider the role of obliquity in Cenozoic icehouse modelling, their efforts are seminal in the study of the connection between orbital forcing and sea-level change at this important temporal bandwidth (Al-Husseini and Mattews, 2010; Mattews and Al-Husseini, 2010).

In this study, we show a good correspondence between well-defined third-order depositional sequences and astronomical cycles. Specifically, we show that icehouse third-order sequences correlate to ~1.2-myr obliquity cycles via glacioeustasy, while greenhouse sequences correspond, in part, to ~2.4-myr eccentricity cycles associated with low-amplitude eustatic change ascribed to glacioeustasy and/or other climatic processes. At the same time, we do not rule out possible contributions from other drivers of sea-level change (e.g., tectonics), particularly for relative sea-level variations.

2. Long-period orbital modulation cycles

Due to gravitational planetary motions and their mutual interaction, the elliptical elements of the orbit of the Earth slowly change through time, resulting in quasi-periodic oscillations in Earth's orbital parameters (eccentricity, obliquity, and climatic precession). These changes control variations in the insolation received on the Earth's surface, which in turn induce climatic variations "fingerprinted" in the sedimentary record (Hays et al., 1976; Imbrie et al., 1984). The eccentricity of the ellipse of the Earth's orbit varies with major periods of ~100 and 405 kyr. The obliquity of the Earth's axis oscillates with a main period of about 40 kyr. Finally, climatic precession varies with an average main periodicity of around 20 kyr.

An important feature of the Earth's orbital parameter variations is that they display modulations in amplitude and frequency. The modulation terms arise through the interference of individual cycles to produce "resultants", with periods ranging from hundreds of thousands to millions of years. The significance of certain amplitude modulation cycles was first described by Laskar (Laskar, 1990, 1999; Laskar et al., 1993), and an extensive review was also given by Hinnov (2000). The most well known long-period modulation cycles are those of eccentricity (~2.4 myr) and obliquity (~1.2 myr). The ~1.2- and ~2.4-myr periods could derive from the interfering terms ~41 kyr (p + s3) and ~39 kyr (p + s4), and ~95 kyr (g4 – g5) and ~99 kyr (g3 – g5), respectively (where p is the Earth's axial precession frequency; s3, s4 are related to the precession of nodes of the Earth and Mars, g3, g4 and g5 are related to the precession of perihelions of the Earth, Mars and Jupiter, respectively, for detail see e.g., Laskar et al., 2004). Thus, the ~1.2- and ~2.4-myr cycles correspond to the fundamental secular frequencies (s3 – s4) and (g4 – g3), respectively.

The orbital motion in the solar system has been demonstrated to be chaotic because of the presence of multiple secular resonances in the inner solar system (Laskar, 1989, 1990). As a result, the orbits of planets undergo slow but non-regular variations. Nevertheless, the 405-kyr periodicity was demonstrated to be relatively stable (Laskar et al., 2004) because it is caused by the gravitational interaction of Jupiter and Venus (i.e., g2 – g5), and Jupiter has an extremely stable orbit. However, the ~1.2- and ~2.4-myr periodicities are not stable, because they result from the motions of the inner planets (the Earth and Mars), which are less regular. An important resonance in this interaction between the motions of perihelions and nodes in the orbital relation of Mars and the Earth is related to a transition from (s4 – s3) – 2(g4 – g3) to (s4 – s3) – (g4 – g3) secular resonance (Laskar, 1990), that links the ~1.2-myr obliquity (s4 – s3) to the ~2.4-myr eccentricity (g4 – g3) modulation cycles. Thus, the unstable ~1.2- and ~2.4-myr periodicities may be considered to be within the same frequency range for the definition of eustatic hierarchies (Section 5.2).

Interestingly, long-period cyclicities in obliquity (~1.2 myr) and eccentricity (405 kyr and ~2.4 myr), have been well recognized in various sedimentary records, and apparently have a significant influence on global climate (e.g., Beaufort, 1994; Olsen and Kent, 1999; Zachos et al., 2001a,b; Pälike et al., 2004, 2006a,b; Wade and Pälike, 2004; Mitchell et al., 2008) and sea-level change (e.g. Lourens and Hilgen, 1997; Strasser et al., 2000; Gale et al., 2002; Matthews and Frohlich, 2002; Boulila et al., 2008a, 2010b; Lirer et al., 2009; Huang et al., 2010a). In this study, we discuss the impact of long-period orbital modulations on global sea level (eustasy) during both Cenozoic icehouse and Mesozoic greenhouse eras.

3. Long-period (~1.2 myr) obliquity modulations correlate to third-order eustatic sequences in the Cenozoic icehouse world

The New Jersey passive margin (North America) was selected by the Ocean Drilling Program (ODP) as an excellent location to investigate the Late Cretaceous to Miocene history of sea-level change because of its rapid sedimentation, tectonic stability, good chronostratigraphic control, and abundant seismic well log and borehole data (Miller and Mountain, 1996). The "New Jersey Sea-Level Transect", an area sensitive to sea-level fluctuations, was designed as a series of boreholes from the onshore New Jersey Coastal Plain across the continental shelf to the slope and rise. In the past decade, extensive work on the Transect allowed improved sequence stratigraphic resolution (e.g., Miller et al., 1998; Pekar et al., 2002). Particularly, the middle Miocene-Oligocene sequences were the subject of high-resolution studies because of their relatively continuous sedimentation and recovery, with excellent chronostratigraphic and paleoenvironmental constraints. Paleocene-Eocene sequences were also studied on the New Jersey margin (Browning et al., 1996; Harris et al., 2010), and sequence boundaries correlate with $\delta^{18}O$ increases in the middle to late Eocene nascent icehouse (Browning et al., 1996). However, global $\delta^{18}O$ amplitudes in the early Eocene are low (i.e., < 0.3‰) and are near detection limits; thus, meaningful comparisons with sequence boundaries and $\delta^{18}O$ are not possible. A more recent comparison suggests a correlation of sequence boundaries and deep-sea oxygen isotopic increases during the Paleocene (Harris et al., 2010). Finally, Pliocene to Pleistocene strata were not studied in

New Jersey because they are difficult to date, and do not form a continuous record there (Miller et al., 1998). Thus, for the Pliocene-Pleistocene we cite studies from equatorial Atlantic and Pacific and the Mediterranean (Lourens and Hilgen, 1997). Then, we tested possible link between ~1.2 myr obliquity cycles and long-term eustatic variations, inferred from $\delta^{18}O$ data (Miller et al., 2005a).

We chose the New Jersey margin for the following reasons:

- The region contains abundant data and rigorous published studies that led to improvement and well-defined Cenozoic third-order eustatic sequences (duration and amplitudes).
- Third-order depositional sequence boundaries were well dated in onshore New Jersey coreholes using biostratigraphy, Sr-isotope stratigraphy (for the late Eocene-Miocene and Campanian-Maastrichtian), and limited magnetostratigraphy (primarily early to middle Eocene). Age resolution is generally better than 1 Myr (viz., better than ±0.5 Myr). Intervals with poorer resolution include the Turonian-Coniacian, middle Campanian, and late middle to late Miocene, where resolution can be as poor as ±1 Myr (Miller et al., 2005a). Late Eocene to early Miocene resolution is as good as 0.5 Myr (viz., ±0.25 Myr; Pekar and Miller, 1996; Miller et al., 2005a).
- Third-order depositional sequence boundaries were demonstrated to be global by correlation with other margins (e.g., Browning et al., 1996; Miller and Mountain, 1996; Pekar and Miller, 1996; Miller et al., 2004; Mizintseva et al., 2009; Harris et al., 2010) and the sequence boundaries of the cycle chart (Vail et al., 1977; Haq et al., 1987); sequence boundaries were linked to increases in deep-sea $\delta^{18}O$ records (inferred glacio-eustatic increases).
- The large amount of data collected from this single margin provides a testable sea-level record that has advantage over compilations from disparate paleogeographic settings that are susceptible to larger uncertainties in sequence stratigraphic interpretation and correlation (e.g., discussed in Boulila et al., 2010b).

3.1. Pliocene-Pleistocene

Comparison of $\delta^{18}O$ records from ODP sites (equatorial Atlantic and Pacific and in the Mediterranean) and the cycle chart of Haq et al. (1987), combined with the analysis of the La90 astronomical model of Laskar et al. (1993), led Lourens and Hilgen (1997) to suggest a correlation between third-order glacioeustatic sequences and the ~1.2-myr obliquity cycles. Specifically, Lourens and Hilgen (1997) suggested that maxima in amplitudes of the ~1.2-myr obliquity cycles induce glaciation events, which in turn cause sea-level lowerings (Haq et al., 1987). This hypothesis is inconsistent with the accepted causal relationship between obliquity variations and climate change (e.g., Hays et al., 1976; Zachos et al., 2001b; Wade and Pälike, 2004; Pälike et al., 2006a; and many others). Amplitude minima (nodes) of obliquity should contribute to the formation of ice-sheets. In fact, Lourens and Hilgen (1997) used a reversed obliquity time series inferred from minima of successive ~40-kyr cycles, which led them to an opposite interpretation. Specifically, their main three age points (2.8, 1.7 and 0.7 Ma) that correspond to sequence boundaries of Haq et al. (1987) match weaker obliquity cycles, with the 0.7 and 2.8 Ma ages coincide exactly with minima in the ~1.2-myr obliquity cycles (see Laskar et al., 2004 for example). In summary, Lourens and Hilgen (1997) show evidence of a link between ~1.2-myr obliquity cycles and glacioeustatic third-order sequences in the Pliocene-Pleistocene interval. To further explore this hypothesis, we applied statistical tests to the revised eustatic curve (Miller et al., 2005a). The most constrained interval of sea level estimate (inferred from $\delta^{18}O$) in Miller et al. (2005a) includes the last 9.25 Ma. Because of the '100 kyr Cycle Problem' of the late Pleistocene (amplitudes of $\delta^{18}O$ oscillations are mainly concentrated at 100 kyr band), our analysis is limited to 1 to 9.25 Ma interval (Fig. 1). Spectral analysis highlights obliquity cycle components (Fig. 2A). The 41–39 kyr and ~1.2 myr cycles are highly significant, which are characterized by strong peaks exceeding 99% confidence level (CL). Other weaker and non

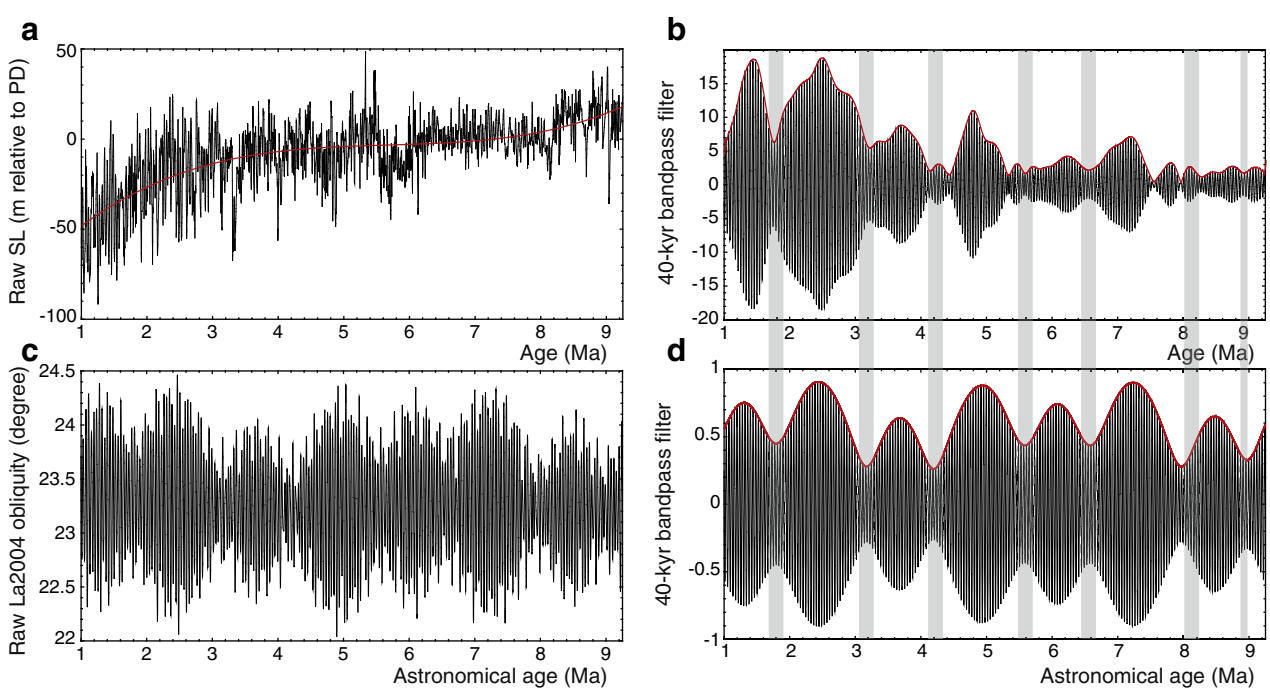

Fig. 1. Amplitude modulation of sea level (SL) variations at obliquity cycle band for 1 to 9.25 Ma interval, and correlation with astronomical obliquity time series. (a) Raw SL estimate inferred from $\delta^{18}O$ (from Miller et al., 2005a), a third-order polynomial fit is also shown. (b) 40 kyr bandpass filter output and Hilbert transformation of 'A'. (c) Raw obliquity time series of La2004 astronomical model (Laskar et al., 2004). (d) 40 kyr bandpass filter output and Hilbert transformation of 'C'. Note that ~1.2 myr obliquity cycles correlates with ~1.2 myr SL minima (see coherency-phase in Fig. 3). As the ~1.2 myr obliquity cycles modulate mainly the ~39 and ~41 kyr cycles (see 'Section 2' for discussion), filtering was performed at 40 kyr band (0.25 ±0.05 cycles/kyr).

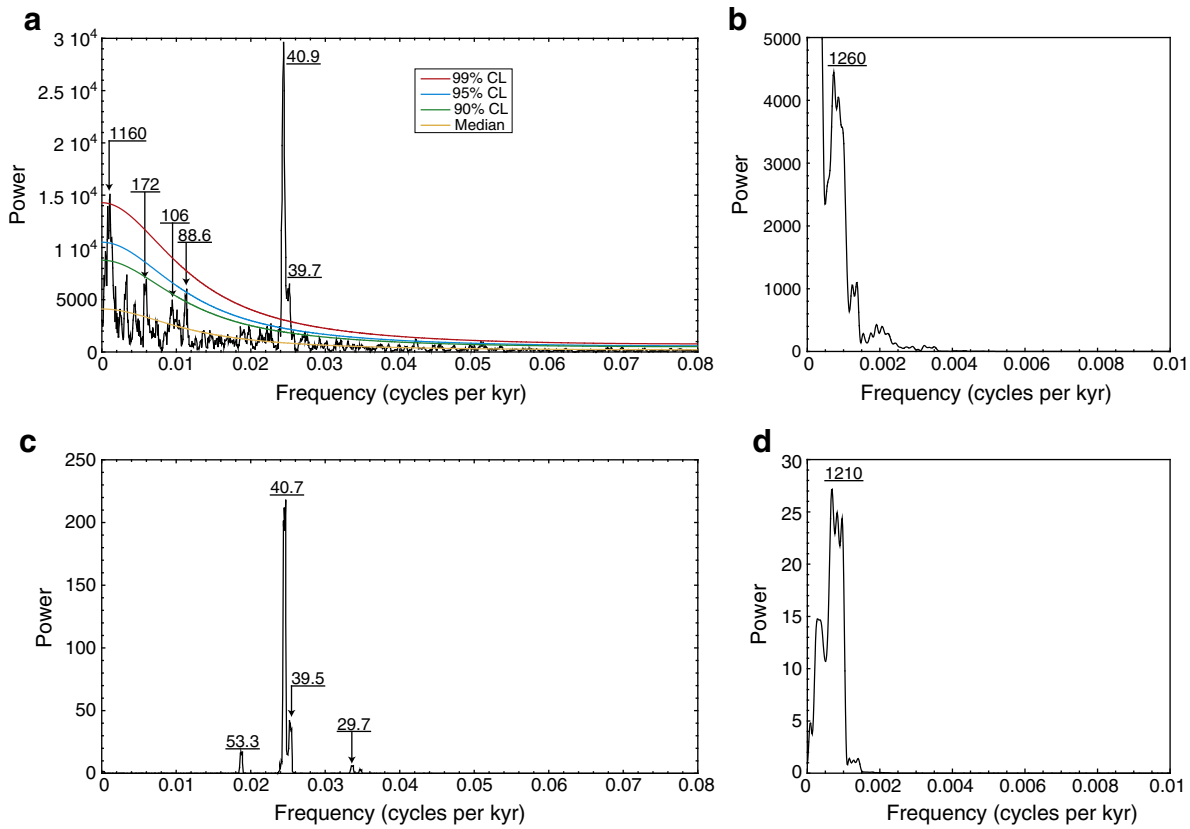

Fig. 2. 2π-MTM power spectra of $\delta^{18}O$ inferred sea level (SL) and La2004 obliquity time series for 1 to 9.25 Ma interval, using the SSA-MTM toolkit (Ghil et al., 2002). (a) Spectrum of detrended SL variations (removed third-order polynomial fit, Fig. 1A). Results of noise modelling (also shown) were estimated using linear fitting and median filtering over 20% of the Nyquist frequency (0.1 cycles/kyr). (b) Spectrum of extracted envelopes of 40 kyr SL oscillations (i.e., Hilbert transformation output of Fig. 1B). Note that a trend of 16-myr peak (power of ~4×10^4), and another high-power (~2.5×10^4) peak at the lowest frequency (4.26-myr period) are truncated to emphasize the 1.2-myr peak. (ca) Spectrum of raw obliquity time series (Fig. 1C). (d) Spectrum of extracted envelopes of 40 kyr obliquity time series (i.e., Hilbert transformation output of Fig. 1D). Note a strong peak of a period of ~1.2 myr is present in SL (Figs. 1B and 2B) and obliquity (Figs. 1D and 2D) as the modulator of 39–41 kyr cycles. All peaks are labelled in kyr.

significant peaks are centered on 88.6, 106, and 172 kyr. The latter is well detected in amplitude modulation (AM) of higher frequency obliquity cycles (e.g., Shackleton et al., 1999). The 88.6 and 106 kyr peaks may correspond either to other obliquity modulation cycles (e.g., Hinnov, 2000) or to weaker eccentricity cycles. Spectrum of the La2004 raw obliquity time series (Fig. 2C) shows, however, only higher frequency cycles (29.7, 39.5, 40.7, and 53.3 kyr) since the lower frequency cycles (e.g., ~1.2 myr) act as modulators (Fig. 1C). To test possible link between lower frequency eustatic sequences and ~1.2 myr obliquity cycles, which is the objective of this section, we performed AM technique on both eustatic and obliquity signals (Figs. 1B,D, 2B,D, and 3). AM of ~39 and ~41 kyr carrier cycles (Figs. 1B,D and 2B,D) shows significant ~1.2 myr cyclicity (see 'Section 2' for astronomical origin) in both eustatic and astronomical signals. The ~1.2 myr eustatic and obliquity cyclicities correlate very well, except in the older part of the studied interval (almost 7.5 to 9.25 Ma), where $\delta^{18}O$ inferred eustatic amplitudes are weak (Section 3.2). Interestingly, ~1.2 myr obliquity nodes coincide with minima of eustatic cycles (Figs. 1B,D and 3), hinting at lower-frequency obliquity pacing of glacioeustatic cycles. These results should, however, be compared to future sequence stratigraphic studies in order to better test the hypothesis of a link between the ~1.2-myr obliquity cycles and third-order sea level during these uni- and bipolar icehouse periods.

3.2. Middle Eocene-Miocene

Comparing onshore and offshore New Jersey sequences with $\delta^{18}O$ records shows that sequence boundaries from 42 to 8 Ma correlate with global $\delta^{18}O$ increases, other sites, and the Haq et al. (1987) cycle chart, linking them with glacioeustatic sea-level lowerings (Miller et al., 1998).

Fourteen Miocene third-order sequences were recognized in the New Jersey margin (Miller et al., 1998, De Verteuil, 1997, Fig. 4 and Table 1). Similarly, the Miocene deep-sea $\delta^{18}O$ record is punctuated by fourteen episodes of increased values known as the Mi events (Miller et al., 1991, 1998, Fig. 4 and Table 1). These oxygen isotopic

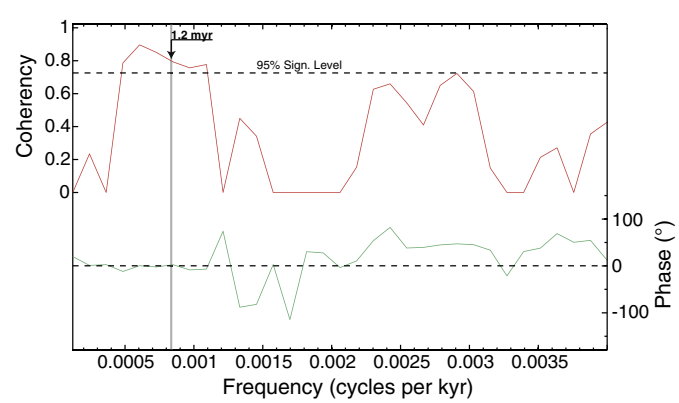

Fig. 3. Coherency and cross-phase spectral analysis of envelopes of 40 kyr sea level (SL) oscillations (Fig. 1B) versus envelopes of 40 kyr obliquity cycles (Fig. 1D). We used the cross-MTM method in Matlab routine of Peter Huybers (e.g., Huybers and Denton, 2008). Note that SL and obliquity are very coherent at ~1.2 myr cyclicity, and that ~1.2 myr SL oscillations are in phase with ~1.2 myr obliquity cycles (indicated by vertical grey bar), i.e., nodes in ~1.2 myr obliquity cycles correlate with minima of ~1.2 myr SL cycles (see Fig. 1).

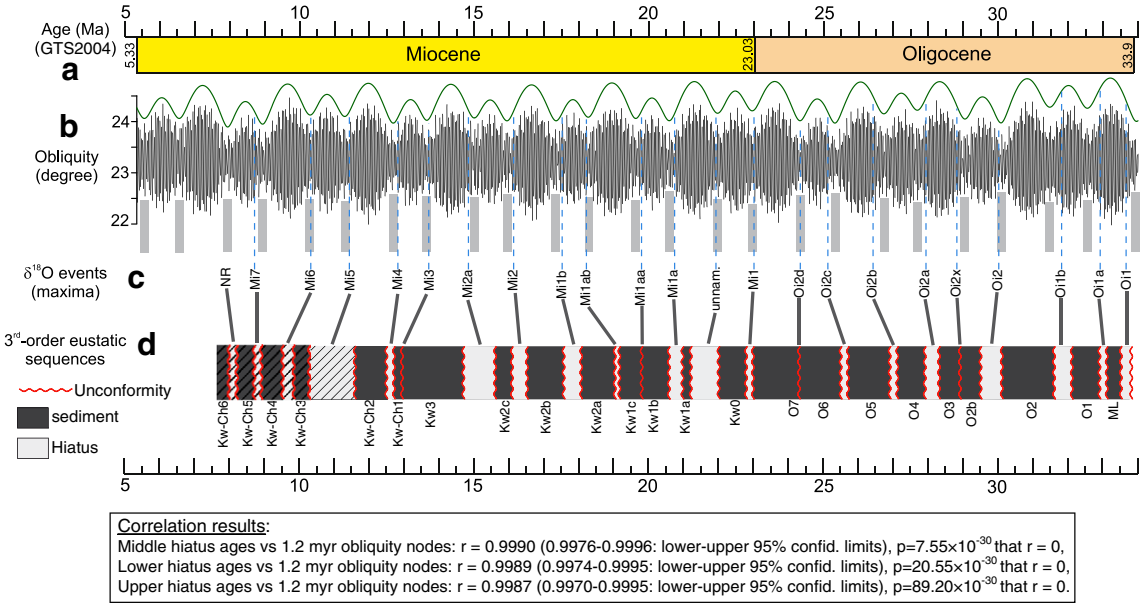

Fig. 4. Correlation between Oligocene through Miocene (~34 to ~5 Ma) third-order eustatic sequences of the New Jersey margin (North America), and long-period (~1.2 myr) obliquity modulation cycles. Sequence boundaries correlate to minima of ~1.2 myr obliquity cycles. (a) Oligocene-Miocene time scale from GTS2004 (Gradstein et al., 2004). (b) Obliquity variations from La2004 model (Laskar et al., 2004), along with the ~1.2-myr envelopes of obliquity. (c) $\delta^{18}O$ events of Miller et al. (1991, 1998). (d) New Jersey third-order sequences (see Table 1 for detail, and references therein). Cross-hatched sequences (Kw-Ch3 to 5) are poorly dated. Vertical bars are located at the long-period (~1.2-myr) obliquity minima (nodes), match most $\delta^{18}O$ event ages (represented by the vertical dashed lines, Table 1) through the Miocene-Oligocene (see text for discussion). Moreover, sequence boundaries correlate well with $\delta^{18}O$ events (e.g., Miller et al., 1998). Phase shifts between ~1.2-myr obliquity nodes and $\delta^{18}O$ events/sequence boundaries may be due to age uncertainties in either $\delta^{18}O$ events or sequence boundaries (see text for discussion). Calculated correlation coefficients between sequence boundaries and ~1.2-myr obliquity nodes are also shown.

shifts have been ascribed to a combination of glacioeustatic sea-level lowering and bottom water cooling of 1–2 °C, but are primarily related to the waxing and waning of the Antarctic ice-sheet (Miller et al., 1991). The $\delta^{18}O$ glacial events were shown to be paced by low insolation episodes during nodes of long-period (~1.2 myr) obliquity cycles (e.g., Holbourn et al., 2007, Fig. 5). Except in the latest Miocene where

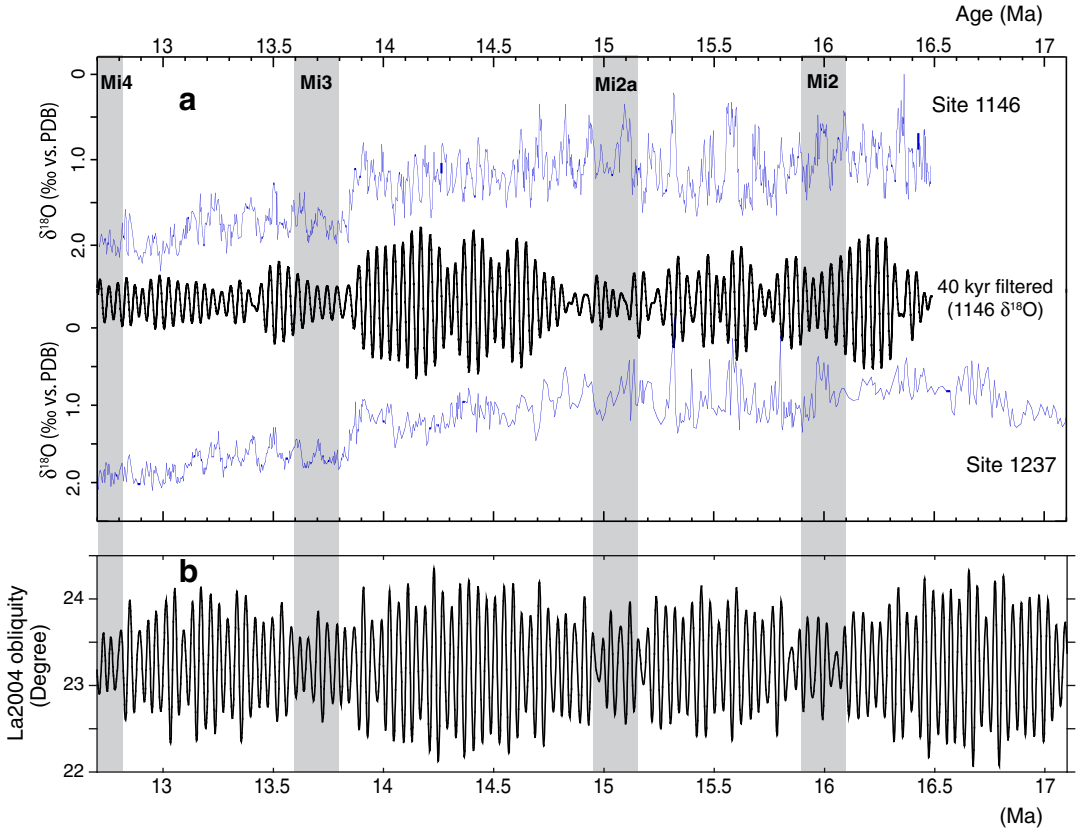

Fig. 5. Correlation of Miocene deep-sea stable oxygen isotopes ($\delta^{18}O$) with obliquity variations (modified from Holbourn et al., 2007). **(A)** Benthic foraminiferal $\delta^{18}O$ of ODP Site 1146 (Northwestern Pacific), its 40 kyr filtered time series, and benthic foraminiferal $\delta^{18}O$ of ODP Site 1237 (Southeastern Pacific). **(B)** La2004 obliquity time series (Laskar et al., 2004). The $\delta^{18}O$ events (e.g., Miller et al., 1998, Table 1) are shown by shaded area, which coincide with minima (nodes) in the ~1.2 myr obliquity cycles (Holbourn et al., 2007).

low-amplitude oscillations of $\delta^{18}O$ can not be correlated worldwide (e.g., Shackleton and Hall, 1997; Anderson and Jansen, 2003, Fig. 1), sequence boundaries, $\delta^{18}O$ events, and ~1.2-myr obliquity nodes (minima) show a good correlation (Fig. 4, Discussion below), pointing to obliquity pacing of glacioeustatic sea-level change.

The Oligocene (23.03 to 33.9 Ma, GTS2004, Gradstein et al., 2004) contains eight $\delta^{18}O$ events (Oi1a, Oi1b, Oi2, Oi2x, Oi2a, Oi2b, Oi2c, and Oi2d, Table 1) and is delimited by two others, the Oi1 and Mi1 events at its lower and upper boundaries, respectively (Fig. 6). All of these $\delta^{18}O$ events correspond to sea-level lowstands of third-order sequences (Fig. 4, Pekar and Miller, 1996; Miller et al., 1998; Pekar et al., 2000, 2002; Pekar and Kominz, 2001), corroborating that base level changes were forced by glacioeustasy. Throughout the entire Oligocene, we note the same number of $\delta^{18}O$ events as nodes of long-period (~1.2 myr) obliquity cycles (Figs. 1 and 3). The average periodicity of third-order sequences in this interval is 1.14 myr, which is similar to the average period of the long-term obliquity cycle. Remarkably, applying the La2004 astronomical model (Laskar et al., 2004), the Oligocene time includes nine ~1.2-myr obliquity cycles, and most of these nodes coincide with sequence boundaries. Moreover, Pälike et al. (2006a, their Fig. 1) showed that major glacial events spanning the Oligocene were mainly paced by obliquity induced insolation/climate in tune with ~1.2 myr cycle nodes.

To further explore this hypothesis, we applied filtering and spectral analysis to $\delta^{18}O$ data, and cross-correlated lower frequency $\delta^{18}O$ variations (those bounded by 'Oi' events) to the ~1.2 myr obliquity cycles (Fig. 6). Lowpass filtering highlights long-term irregular $\delta^{18}O$ variations that dominate the spectral powers (Spectrum of Fig. 1d), and a significant shorter cyclicity of a mean periodicity of 1.05 myr (Fig. 6d). Bandpass filtering further highlights the myr-scale $\delta^{18}O$ cyclicity. When compared to ~1.2 myr obliquity cycles (Fig. 6c), most of 'Oi' $\delta^{18}O$ events correlate with obliquity minima. 'Oi2d' and 'Oi2c' $\delta^{18}O$ events do not show correlation with ~1.2 myr obliquity nodes ('question marks' in Fig. 6b) neither in lowpass nor in bandpass filtering. This mismatch may be explained by the fact that the interval ~23 to ~27 Ma, including 'Oi2d' and 'Oi2c' events, records a pronounced multi-myr $\delta^{18}O$ cycle that may mitigate amplitudes of myr-scale cycles (Fig. 6b, lowpass filtering). Nevertheless, the 'Oi2d' and 'Oi2c' events are visually obvious in the raw $\delta^{18}O$ data (Fig. 6a). Finally, cross-correlation of envelopes of 40 kyr obliquity cycles and myr-scale $\delta^{18}O$ cycles shows a good coherency at ~1 myr, instead of ~1.2 myr, where obliquity nodes match well $\delta^{18}O$ maxima ('Oi' events, Fig. 6e). One remark we have to note is that, compared to Pliocene-Pleistocene (Figs. 1 to 3), cross-correlation does not show flat cross-phase at the ~1.2 myr band (Fig. 3), and the elevated coherency is concentrated at ~1 myr period instead of ~1.2 myr. Currently, we have no explanation for this difference in periodicity between myr-scale $\delta^{18}O$ and astronomical obliquity cycles. Such observation should, however, be considered in future detailed cyclostratigraphic studies of Oligocene $\delta^{18}O$ data. Then, we correlated sequence boundaries and ~1.2 myr obliquity minima of the Oligocene-Miocene interval (Fig. 4). The calculated correlation coefficients 'r' are very high. For example, when ~1.2 myr obliquity minima is correlated to middle hiatus ages (Fig. 4), 'r' is 0.9990 with lower and upper 95% confidence limits of 0.9976 and 0.9996 respectively. Such correlation is highly significant with a very low probability value close to zero when considering the null-hypothesis (i.e., that r = 0). Thus, the close correspondance in number and in timing and the aforhighlighted

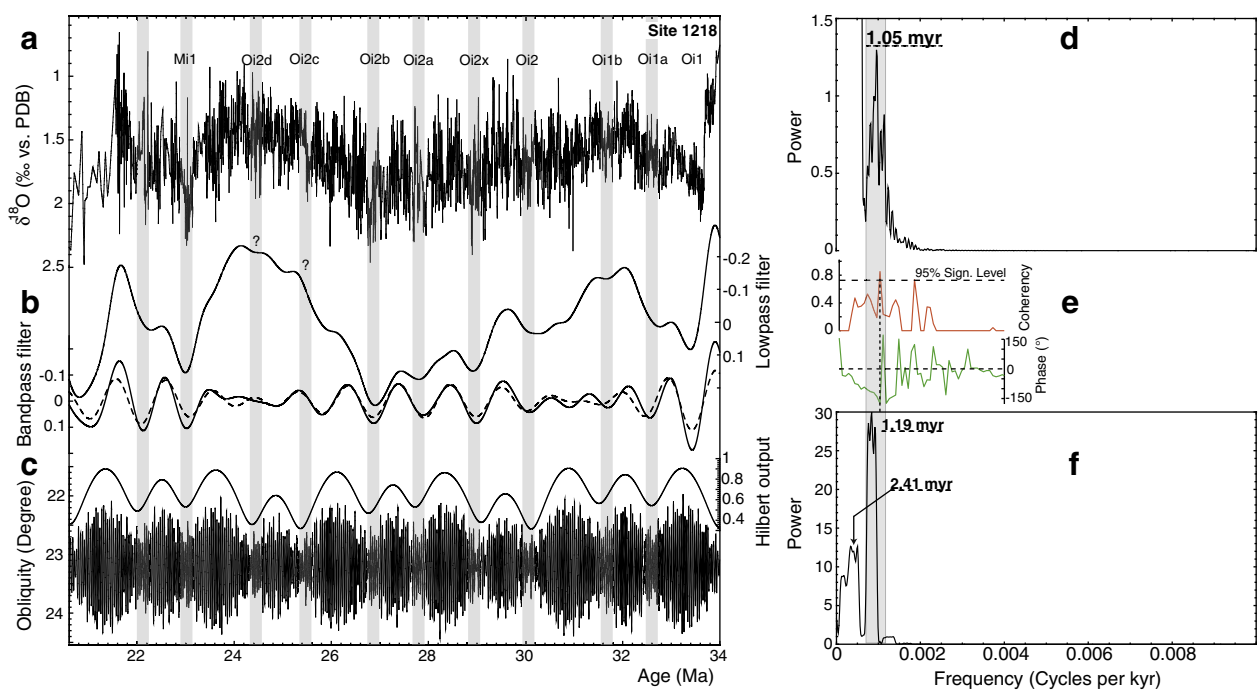

Fig. 6. Correlation of Oligocene deep-sea stable oxygen isotopes ($\delta^{18}O$) with obliquity variations ($\delta^{18}O$ data are from Pälike et al., 2006a). (a) Benthic foraminiferal $\delta^{18}O$ of ODP Site 1218 (Equatorial Pacific), the $\delta^{18}O$ events (e.g., Miller et al., 1998, Table 1) are also shown, which correlate with minima (nodes) in the ~1.2 myr obliquity cycles. Except 'Oi1a' and 'Oi2c' $\delta^{18}O$ events, all other events are also shown by Pälike et al. (2006a) in their Fig. 1. (b) Gaussian filter outputs of $\delta^{18}O$ signal in 'A', upper curve: lowpass filter output (cutoff frequency 1.25 cycles/myr), lower curves: bandpass filter outputs using two bands (solid curve: cutoff frequencies 0.5618 and 1.3618 cycles/myr, dashed curve: cutoff frequencies 0.7618 and 1.1618 cycles/myr). 'Question marks' at 'Oi2d' and 'Oi2c' indicate that filtering process does not succeed in detection of $\delta^{18}O$ maxima, which are visually obvious in the raw $\delta^{18}O$ data (see text for discussion). (c) Raw obliquity time series of La2004 astronomical model (Laskar et al., 2004), and Hilbert transformation output of the filtered obliquity series to 39–41 kyr band (cutoff frequencies 0.023 and 0.027 cycles/kyr). (d) 2pi-MTM power spectrum of lowpass filterd $\delta^{18}O$ time series in 'B'. Note that the high-power (~24) peak at the lowest frequency (5.23-myr period), and other low-frequency peaks (2.52, 2.02, 1.7 myr) are truncated to emphasize the myr-scale peak. (e) Coherency and cross-phase spectral analysis of lowpass filtered $\delta^{18}O$ in 'B' versus Hilbert transformation output in 'C' (i.e., envelopes of 40 kyr obliquity cycles). Vertical dashed line indicates high coherency at ~1 myr. (f) 2pi-MTM power spectrum of Hilbert transformation output in 'C'. Note that $\delta^{18}O$ and obliquity are coherent at ~1 myr cyclicity, but not at ~1.2 myr (see text for discussion), and that $\delta^{18}O$ oscillations and obliquity cycles are antiphased (−180° cross phase at ~1 myr), i.e., nodes of obliquity cycles correlate with maxima of $\delta^{18}O$ cycles (see 'B'). For cross-correlation, we used the cross-MTM method in Matlab routine of Peter Huybers (e.g., Huybers and Denton, 2008).

significant correlation between most of eustatic sequence boundaries, $\delta^{18}O$ events, and ~1.2-myr obliquity nodes provides compelling evidence for a link between them.

The Alabama St. Stephens Quarry (southern US) (Miller et al., 2008) is another site that contains well-constrained third-order sequences from the late Eocene to early Oligocene (~30 to ~36 Ma). These sequences correlate well with the New Jersey E10, E11, ML, O1, and O2 sequences, and with global $\delta^{18}O$ increases, also suggesting that glacioeustasy is the primary mechanism responsible for forming sequence boundaries not only in the Oligocene, but also in the late Eocene "greenhouse" (discussion below). The average duration of glacioeustatic sequences of this late Eocene to early Oligocene interval (~30 to ~36 Ma) is ~1.2 myr, which is equal to the average obliquity modulation cycle. Also, we note the same number of sequences and astronomical cycles. Moreover, four of six sequence boundaries match the ~1.2 myr obliquity nodes of La2004 model well. We interpret this correspondence between third-order sequences and ~1.2-myr obliquity cycles to indicate that obliquity forcing is the major control on glacioeustatic change and sequence boundary formation for the period between 42 and 8 Ma.

3.3. Paleocene-Eocene

The Paleocene and Eocene New Jersey sequences are less constrained than Oligocene and Miocene sequences due to less precise chronostratigraphy, lower sequence stratigraphic resolution, and $\delta^{18}O$ variations of lower amplitudes precluding a possible correlation. Miller et al. (1998) recognized three third-order sequences for the entire Paleocene, labelled Pa1, Pa2, and Pa3. Ten years later, owing to new coreholes and improved dating, Kominz et al. (2008) and Harris et al. (2010) identified seven Paleocene sequences (Table 2). For the Eocene, Miller et al. (1998) recognized eleven third-order eustatic sequences in New Jersey. More recently, from South Tasman Rise coreholes (ODP Leg 189, Site 1171) with well-constrained dating and through a correlation with the New Jersey sequences, Pekar et al. (2005) proposed an additional sequence between the E7 and E8 New Jersey sequences (Table 2). Likewise, in their backstripped sea-level estimates Kominz et al. (2008) presented an additional sequence between E5 and E6 (E6a, in their Fig. 8). Therefore, compiled data from Browning et al. (1996), Miller et al. (1998), Pekar et al. (2005), Kominz et al. (2008), and Harris et al. (2010) present a more complete Paleocene-Eocene eustatic sequence framework (Table 2). Paleocene and Eocene sequence boundary ages have approximately ±1-myr and ±0.5-myr uncertainties, respectively (Miller et al., 1998). New Jersey Paleocene-Eocene sequences correlate with several worldwide sequences, indicating a global sea-level control (Browning et al., 1996; Miller et al., 1998; Pekar et al., 2005; Kominz et al., 2008).

As mentioned above, New Jersey sequence boundaries from 42 to 8 Ma (late Eocene to Oligocene) correlate to global $\delta^{18}O$ increases, linking them with glacioeustatic sea-level lowerings (e.g., Browning et al., 1996; Miller and Mountain, 1996; Miller et al., 1998). More recently, Pekar et al. (2005) extended the correlation (i.e., sequence boundaries and $\delta^{18}O$ increases correlation) to 51 Ma (early to middle Eocene, 51–42 Ma), suggesting that the development of the Antarctic ice sheet occurred at ca. 51 Ma, and may mark the beginning of the 'icehouse' world.

As the existence of significant ice sheets is uncertain for the Early Eocene through Paleocene, we compared third-order eustatic sequences with both ~1.2- and ~2.4-myr astronomical cycles (Table 2) for these time intervals. Paleocene and Early Eocene sequences in New Jersey do not show an obvious match to either the obliquity or the eccentricity modulation cycles. Specifically, the Paleocene interval (55 to 64.5 Ma) includes seven third-order sequences (Harris et al., 2010), this interval corresponds to four ~2.4-myr eccentricity cycles, and eight ~1.2-myr obliquity cycles. However, the New Jersey Paleocene section has several long hiatuses (Browning et al., 1996; Harris et al., 2010), which may explain the apparent mismatch. Also, twelve sequences are observed in the Eocene interval (33 to 55 Ma), while the La2004 model predicts eighteen obliquity cycles and nine eccentricity cycles. Additionally, several long (1–2 myr) Eocene hiatuses exist that may span sequences that have not been recognized on this margin.

Focusing on the relatively well-defined sequences from the South Tasman Rise (Pekar et al., 2005), in comparison with long-period obliquity modulation cycles yields additional insights (Fig. 7). Pekar et al. (2005) correlated their South Tasman Rise sequence boundaries to deep-sea $\delta^{18}O$ increases (Table 2). Four of six sequence durations (Yp4, Yp5, Lu1, Lu3) fall exactly in the long-period obliquity modulation band (1.4, 1.3, 1.3, and 1.4 myr, respectively). Even if the Lu2 sequence duration (2.6 myr) falls in the eccentricity band, this sequence could be divided into two sequences. In fact, variations in the proxies used for that interpretation (Pekar et al., 2005, their Fig. 3) are below the resolution of these methods. For example, planktonic/benthic (P/B) ratios and carbonate content (%$CaCO_3$) are very low, and show no significant variations in the middle to upper part of sequence Lu2 (e.g., zero %$CaCO_3$ in the upper part). Moreover, the $\delta^{18}O$ data used to support their interpretation present the lowest resolution in this interval. In sum, we infer that obliquity forcing is the main astronomic driving force of middle-late Eocene eustatic sequences. Additional evidence of orbital forcing is seen in sequence Lu1 (Fig. 7). This sequence was delineated by several proxies (palaeontological, sedimentological, and physico-chemical proxies, Fig. 7). Its duration was estimated by biostratigraphy and magnetostratigraphy as 1.4 myr (47.1 to 48.5 Ma), and by correlation with $\delta^{18}O$ to only 1.2 myr (46.9 to 48.1 Ma). This duration is equal to the average obliquity period (i.e., ~1.2 myr), and may correlate to a ~1.2-myr astronomical cycle in the La2004 model (Fig. 7). Given uncertainties in GTS2004 and the not yet established ATS (astronomical time scale), we consider that this correlation between nodes and sequence boundaries in Fig. 7 is very preliminary. It corresponds to a floating correlation/timescale (e.g., Laskar et al., 2004; Hinnov and Ogg, 2007) rather than an absolute correlation. Interestingly, the photospectrometry record clearly documents 6 shorter sequences within Lu1, with an

Table 2
Compiled Paleocene-Eocene sequence stratigraphic data from New Jersey and the South Tasman Rise from Browning et al. (1996), Miller et al. (1998), Pekar et al. (2005), and Kominz et al. (2008). Alternative data in parentheses are from the South Tasman Rise (ODP Site 1171, Leg 189, Pekar et al., 2005). Ei10* and Ei12* are $\delta^{18}O$ events that were unnamed in Miller et al. (1998). NR indicates that results were not recognized in the New Jersey margin. Paleocene-Eocene sequences were rescaled to GTS2004 (Gradstein et al., 2004).

3rd order sequence	Basal sequence bounday/Hiatus age (Ma)	d18O event	d18O maximum age (Ma)
E11	34.35	Ei12*	34.1
E10b	35.54-35.72		
E10a	36.32-36.24	NR	
E9	39.1-37.0	Ei10*	39.9
E8(Lu4)	41.93-41.37	Ei9	41.9(42.8)
NR(Lu3)	NR(44.5)	Ei8	NR(44.2)
E7(Lu2)	45.17-43.72(47.1)	Ei7	44.4(46.9)
E6(Lu1)	46.54-45.28(47.8-48.5)	Ei6	47.5(48.1)
E5(Yp5)	49.16-48.07(49.2)	Ei5	48.1(49.4)
E4(Yp4)	50.75-50.51(50.9)	Ei4	50.6(50.8)
E3	53.16-52.57		52.4
E2	54.54-54.09		54
E1	55.54-55.32		55.6
PaA	56.44-56.32		
PaB	57.91-57.39		
PaC	58.72-58.32		
PaD	60.47-59.40		
PaE	61.82-60.76		
PaF	62.83-62.37		
PaG	64.9-63.55		

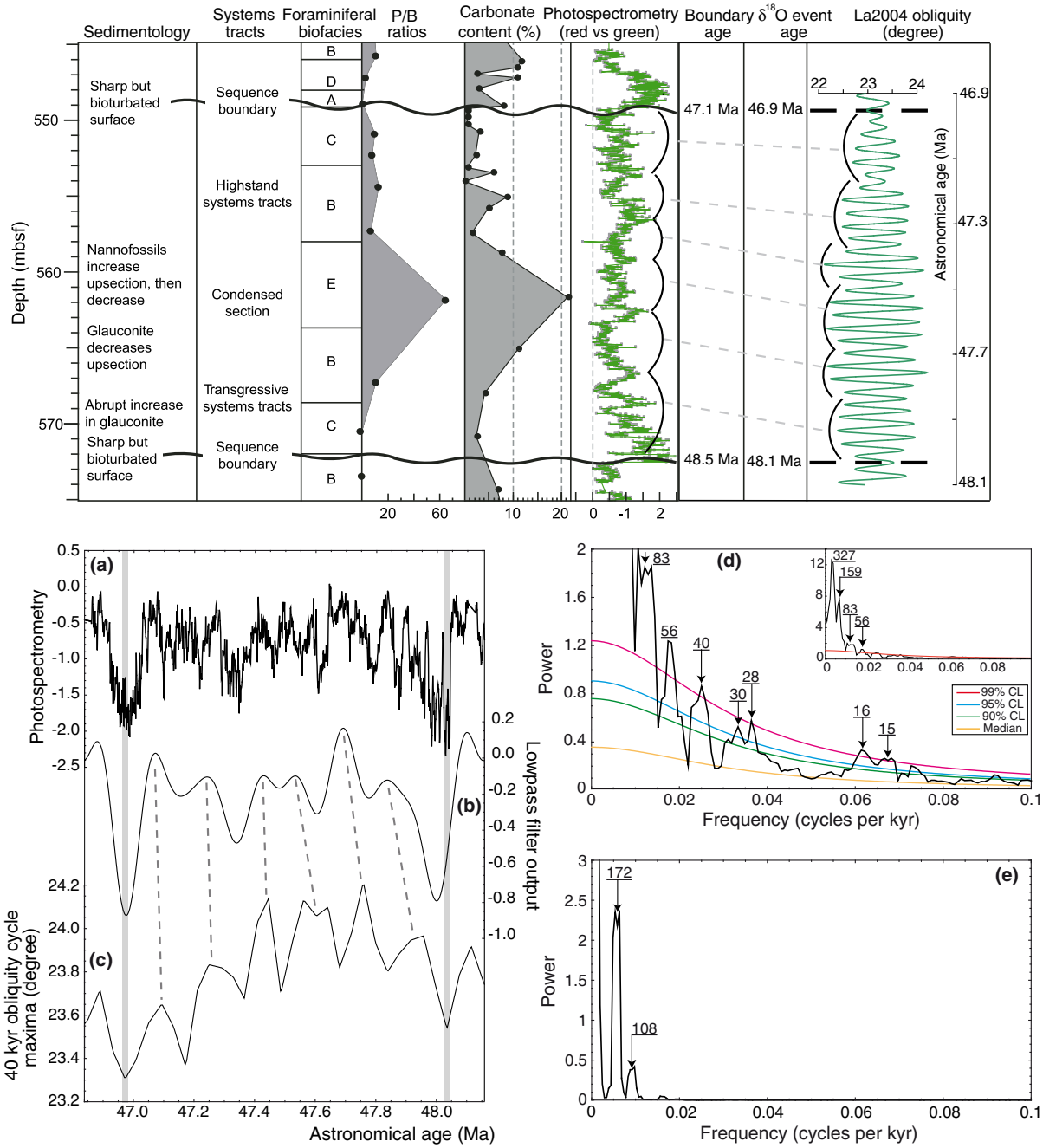

Fig. 7. Upper panel: detailed third-order glacioeustatic sequence (Lu1) defined by several approaches: sedimentology, planktic/benthic foraminiferal ratios (P/B), carbonate content, and rock color at South Tasman Rise, ODP Site 1171, Leg 189, middle Eocene (Pekar et al., 2005). The sequence is bounded by bioturbated surfaces. Two $\delta^{18}O$ events occurring at 46.9 Ma and 48.1 Ma, closely match sequence boundaries. These latter appear to match the ~1.2-myr obliquidy nodes of the La2004 model (Laskar et al., 2004). Also, the photospectrometry curve exhibits higher frequencies that most likely correspond to obliquity components (see text for discussion). Lower panel: spectral analysis and filtering results of photospectrometry data. (a) Time-calibrated photospectrometry data by matching sequence boundaries into two age points (46.97 and 48.03 Ma) corresponding to long-term obliquity cycle minima (see 'lower panel' and 'C'). (b) Lowpass filtering of 'A' using Taner filter (Taner, 2000) to isolate 160–200 kyr and 1.2 myr obliquity modulation cycles ((cutoff frequency 0.008 cycles/kyr). (c) Generated obliquity time series by extraction of maxima values of the 40 kyr cycles. Vertical grey-shaded bars indicate sequence boundaries, higher frequency (160–200 kyr) obliquity modulation cycles that may correspond to higher frequency photospectrometry cycles are also shown by dashed lines. Note that this correlation and the tuning in 'A' is a simple floating timescale because uncertainties in geological timescale does not presently allow any direct correlation (see text for discussion). (d) 2pi-MTM power spectrum of the time-calibrated photospectrometry data in 'A' using the SSA-MTM toolkit (Ghil et al., 2002). Results of noise modelling (also shown) were estimated using linear fitting and median filtering over 20% of the Nyquist frequency (0.5 cycles/kyr). Note that the high-power (~14) peak at the lowest frequency (327-kyr period), and another low-frequency peak (159 kyr) are truncated to emphasize the higher frequency peaks, see the *inset* zoom in, that corresponds to the original spectrum. (e) 2pi-MTM power spectrum of 'C'.

average duration of ~160 kyr (Fig. 7). This period corresponds closely to the short obliquity modulation periodicity (i.e., ~160- to ~200-kyr periodicity, Fig. 7, e.g., see Shackleton et al., 1999; Hinnov, 2000). Other shorter oscillations are visible, which may include some correspondence with the ~40-kyr obliquity cycles (Fig. 7). These observations are highlighted by filtering and spectral analysis (Fig. 7) as follows. Spectral analysis shows evidence of the three main obliquity components (56, 40 and the averaged 29 kyr). These cyclicities are documented with higher powers compared to possible precession cycles (16 and 15 kyr). A 83-kyr peak may correspond either to eccentricity or obliquity cycle (Fig. 7, lower panel, 'E'). Interestingly, the strong 159-kyr peak corresponds most likely to 172 kyr obliquity

modulation cycle, well detected in the higher frequency (~40 kyr) obliquity cycle maxima (Fig. 7, lower panel, 'E'). Finally, the strongest 327-kyr peak may correspond to harmonic of the 159-kyr cycle (see lowpass filtering in 'B'). We suggest that within the Lu1 third-order sequence of Pekar et al. (2005), obliquity exhibits its frequency range, hinting at a hierarchy of glacioeustastic control on depositional sequences. This supports the hypothesis that third-order glacioeustatic sequences reflect ~1.2-myr obliquity cycles for at least the last 51 Ma, i.e. middle Eocene. Further study of Paleocene to early Eocene sequences are needed to evaluate their global nature and to better constrain their ages.

4. Long-period (~2.4 myr) eccentricity modulations correspond to third-order eustatic sequences in Mesozoic greenhouse world

Several sedimentary records register predominance of precession-eccentricity versus obliquity forcing of sea-level change throughout Mesozoic greenhouse intervals. For the Cretaceous, we mainly illustrate with the well-studied Late Cretaceous of the New Jersey margin, North America (e.g., Miller et al., 2003, 2004). For the Jurassic, we cited three late Jurassic examples from outcrops in Switzerland, Germany, Spain, and France (Strasser et al., 2000; Boulila et al., 2008a, 2010b). Finally, for the Triassic we briefly discuss the lacustrine Newark basin deposits of eastern North America (Olsen and Kent, 1999), and then give some examples of studies on marine deposits.

4.1. Cretaceous

Relatively rigorous and complete Late Cretaceous (65.5 to 99.6 Ma, GTS2004) sea level reconstructions come from studies of the New Jersey record (Miller et al., 2003, 2004, 2005b; Van Sickel et al., 2004; Browning et al., 2008; Kominz et al., 2008; Mizintseva et al., 2009). Fifteen third-order sequences were identified in the New Jersey coastal plain for the interval ~64 to ~99 Ma (Table 3). Sequence boundaries show a strong correlation with sea-level falls of the Haq et al. (1987) cycle chart, northwest European sections, and Russian platform outcrops (Miller et al., 2003, 2004). This correlation points to a global control on the deposition of New Jersey third-order sequences i.e., eustatic control (Miller et al., 2003, 2004). Eustatic estimates were obtained by backstripping, accounting for paleodepth variations, sediment loading, compaction, and basin subsidence (Miller et al., 2004; Kominz et al., 2008). This approach indicates large (>25 m) and rapid (<1 myr) sea-level variations during the Late Cretaceous greenhouse world. Although Late Cretaceous benthic foraminiferal $\delta^{18}O$ records have not attained the resolution needed to test their relationship with sequence boundaries, as has been done for the Oligocene-Miocene, three significant $\delta^{18}O$ increases (71.2, 92–93, and 96 Ma), matching three sequence boundaries (basal Navesink I, basal Bass River III, and basal Bass River I, respectively, Table 3), suggest ephemeral ice sheets in Antarctica, hinting at a glacioeustatic contol of third-order sequences (Miller et al., 1999, 2003, 2004).

The same number of third-order sequences are observed in New Jersey as are seen in the long-period (~2.4 myr) eccentricity cycles of La2004 and La2010d models (Laskar et al., 2004, 2011; Fig. 8). The fifteen third-order sequences of New Jersey span ~64 to ~99 Ma (Miller et al., 2003, Fig. 8 and Table 3). For the same interval, astronomical models predict fifteen long-period (~2.4-myr) eccentricity cycles (Fig. 8 and Table 3). This correspondence in number suggests a possible link. A direct correlation between the two series is not seen, however (Fig. 8). Instead, there is a large difference in the durations of the sequences as compared to the durations of the ~2.4-myr astronomical cycles (Table 3). Moreover, astronomical models are not well constrained in this interval (i.e., ~64 to ~99 Ma, Laskar et al., 2004, 2011), as indicated by the phase shift between La2004 and La2010d orbital eccentricity curves (Fig. 8b,c), and well demonstrated by several astronomical modelling tests (Laskar et al., 2011). The La2004 model was demonstrated as precise for the last 40 Ma (Laskar et al., 2004). La2010d model extends the precision to the last 50 Ma (Laskar et al., 2011).

In New Jersey, these sequence boundary ages (Table 3) were derived from integrating Sr-isotopic and biostratigraphic approaches, with an age error of ±1 myr (Miller et al., 2003). Given these uncertainties and adding uncertainties regarding under- or overestimated hiatus durations, and considering the lack of accuracy in astronomical models beyond 40 to 50 Ma (Laskar et al., 2004, 2011), we suggest that any correspondence between third-order sequences and ~2.4-myr eccentricity cycles (Fig. 8) may suggest a link between the two. This hypothesis is, in fact, supported by several other examples of Mesozoic greenhouse sequences in Jurassic and Triassic (Section 4.2), and in the Aptian cyclostratigraphy. In this latter example, Huang et al. (2010b) showed evidence of strong lower frequency eccentricity cycles from high-resolution grayscale data of the Italian Aptian (Piobbico core, central Italy). Specifically, they showed prominent 405-kyr and ~2-myr eccentricity cycles (their Fig. 2, see Section 5.2), which were correlated to carbonate content variations. These astroclimatic cycles likely reflect sea-level variations (e.g., Fischer, 1986). The ~2.4-myr astronomical cycles could control 'weaker' glacioeustatic change, and/or other drivers of sea-level change (Section 5.1). We suggest that low insolation episodes of amplitude minima in the ~2.4 myr eccentricity cycles induced Antarctic ice sheets, which in turn, caused global sea-level drops, and the formation of sequence boundaries (e.g., Matthews and Frohlich, 2002; DeConto and Pollard, 2003). A preliminary astronomical correlation of New Jersey third-order sequences is possible, within the age uncertainties and astronomical model limitations (Fig. 8). In fact, several boundaries may correspond to minima of ~2.4 myr eccentricity cycles. On the other hand, the mismatch may be due alternate sea-level drivers (e.g., non-orbital climatic processes, tectonics, etc.; e,g., Lovell, 2010, see discussion below).

Table 3
Comparison of ages of Late Cretaceous third-order eustatic sequences of New Jersey, North America (Miller et al., 2003, 2004; Kominz et al., 2008), with long-period (~2.4 myr) eccentricity cycles of the La2004 and La2010d models (Laskar et al., 2004, 2011). Note that we have as much ~2.4 myr cycles as third-order sequences (see text for discussion). LC: Late Cretaceous. Pal: Paleocene. The ~2.4 myr eccentricity minima are inferred from lowpass filtering of the raw eccentricity curves (Fig. 8). Late Cretaceous sequences were rescaled to GTS2004 (Gradstein et al., 2004).

3rd order sequence	Basal sequence boundary/ Hiatus age (Ma)	2.4-myr astron. cycle	La2004/La2010d Minimum age (Ma)	La2004/La2010d Astron. cycle duration (Ma)
Paleocene	64.9-63.55	Pal1	64.347/63.206	
Navesink II	67.14-66.24	LC15	66.722/65.089	2.375/1.883
Navesink I	71.09-69.94	LC14	69.074/68.418	2.352/3.329
Marshalltown	75.96-75.85	LC13	71.397/70.424	2.323/2.006
Englishtown	78.04	LC12	73.318/72.766	1.921/2.342
Merchantville III	83.1-82.2	LC11	75.629/75.106	2.311/2.340
Merchantville II	84-83.9	LC10	78.449/77.318	2.820/2.212
Merchantville I	84.8-84.5	LC9	80.710/79.598	2.261/2.280
Cheesequake	85.2	LC8	82.968/81.624	2.258/2.026
Magothy III	88.3-87.8	LC7	85.230/84.550	2.262/2.926
Magothy II	90-89.8	LC6	87.330/86.600	2.100/2.050
Magothy I	92.1-91.3	LC5	89.683/89.002	2.353/2.402
Bass River III	93.5	LC4	91.707/91.139	2.024/2.137
Bass River II	95.3-95	LC3	94.027/93.246	2.320/2.107
Bass River I	97.5-96.7	LC2	96.286/96.208	2.259/2.962
Potomac	99.6-?	LC1	98.577/98.313	2.291/2.105

4.2. Jurassic -Triassic

High-resolution magnetic susceptibility (MS) variations has been studied in exceptionally exposed sections of Oxfordian and Kimmeridgian outcrops in southeastern France (Boulila, 2008; Boulila et al.,

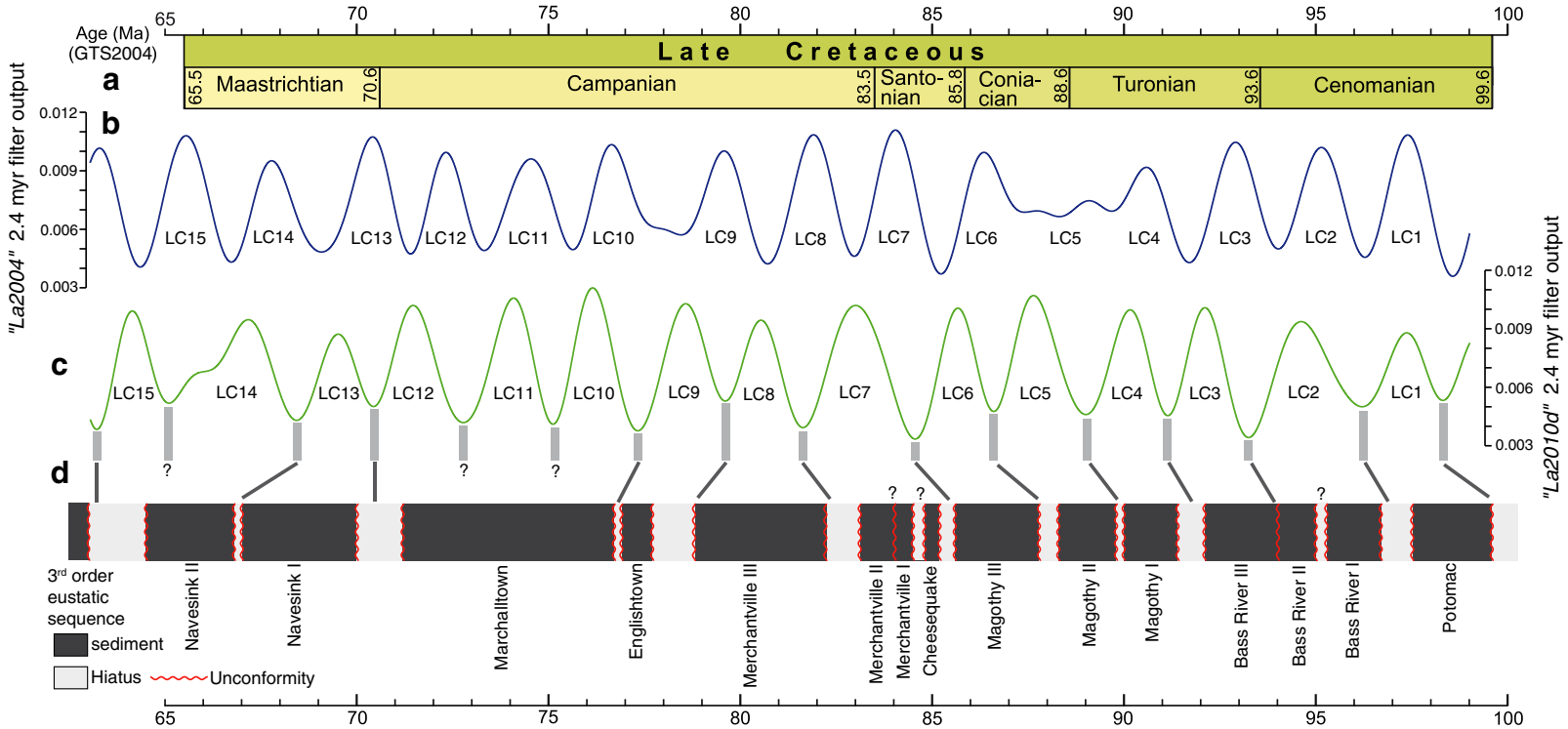

Fig. 8. Comparison of the Late Cretaceous (~64 to ~99 Ma) third-order eustatic sequences of New Jersey (North America) with ~2.4 myr orbital eccentricity cycles extracted by lowpass filtering (Taner, 2000) of the raw eccentricity time series (frequency cutoff 0.7 cycles/myr). Some sequence boundaries may correspond to minima of the long-period (~2.4 myr) eccentricity modulations. **(a)** Late Cretaceous time scale from GTS2004 (Gradstein et al., 2004). **(b)** ~2.4 myr eccentricity cycles of the La2004 astronomical model (Laskar et al., 2004). **(c)** ~2.4 myr eccentricity cycles of the most recent and constrained La2010d astronomical model (Laskar et al., 2011); LC: Late Cretaceous, LC1 to LC15: ~2.4 myr eccentricity cycles. Minima in the ~2.4 myr La2010d eccentricity cycles are indicated by vertical bars, and a possible correspondance with sequence boundaries is shown (see text for discussion). **(d)** New Jersey third-order eustatic sequences (Miller et al., 2003, 2004; Kominz et al., 2008); hiatuse/unconformity ages are given in table 3. Question mark indicates no equivalent sequence boundary can correspond to the ~2.4 myr eccentricity minimum or vice versa.

2008a,b,c, 2010b). The Oxfordian Terres Noires Formation exhibits high sedimentation rates (~150 m/myr) of ammonite-rich marine marls (Boulila et al., 2010b). Time-series analysis of early to middle Oxfordian MS variations in the marls highlighted sub-Milankovitch to Milankovitch climate variations (Boulila et al., 2008c, 2010b). Predominant oscillations related to 405-kyr and ~2-myr orbital eccentricity modulations were demonstrated (Fig. 9). When compared to third-order eustatic sequences as defined in the reference European chart of Hardenbol et al. (1998), the lower ~2-myr MS cycle (labelled S1) corresponds to the Ox0-Ox1 sequence; however the 405-kyr MS cycles (labelled C6 to C9) correlate with third-order sequences (Ox1-Ox2, Ox2-Ox3, Ox3-Ox4, Ox4-Ox5). Thus, third-order sequences sometimes match the ~2-myr, and sometimes correlate with the 405-kyr eccentricity cycles. This confusion in sequence orders was discussed in Boulila et al. (2010b), as deriving from the quality of sections having low sedimentation rates, which were used to establish this portion (Late Jurassic) of the reference chart (Hardenbol et al., 1998). Our results are also supported by Saudi Arabia outcrops (Al-Husseini et al., 2006; Al-Husseini, 2009) as follows. Terres Noires sequence S1 biostratigraphically correlates with the early Oxfordian Hawtah sequence in Saudi Arabia. Importantly, the Hawtah sequence consists of five sea-level cycles, which are correlative to the Terres Noires C1-C5 cycles, and were interpreted as 405 kyr cycles.

MS variations of alternating marl-limestone successions of the French Kimmeridgian exhibit precession index cycles strongly modulated by 405-kyr eccentricity cycles (Fig. 10). The latter correlate well with third-order eustatic sequences of the European reference chart of Hardenbol et al. (1998). An additional sequence boundary between

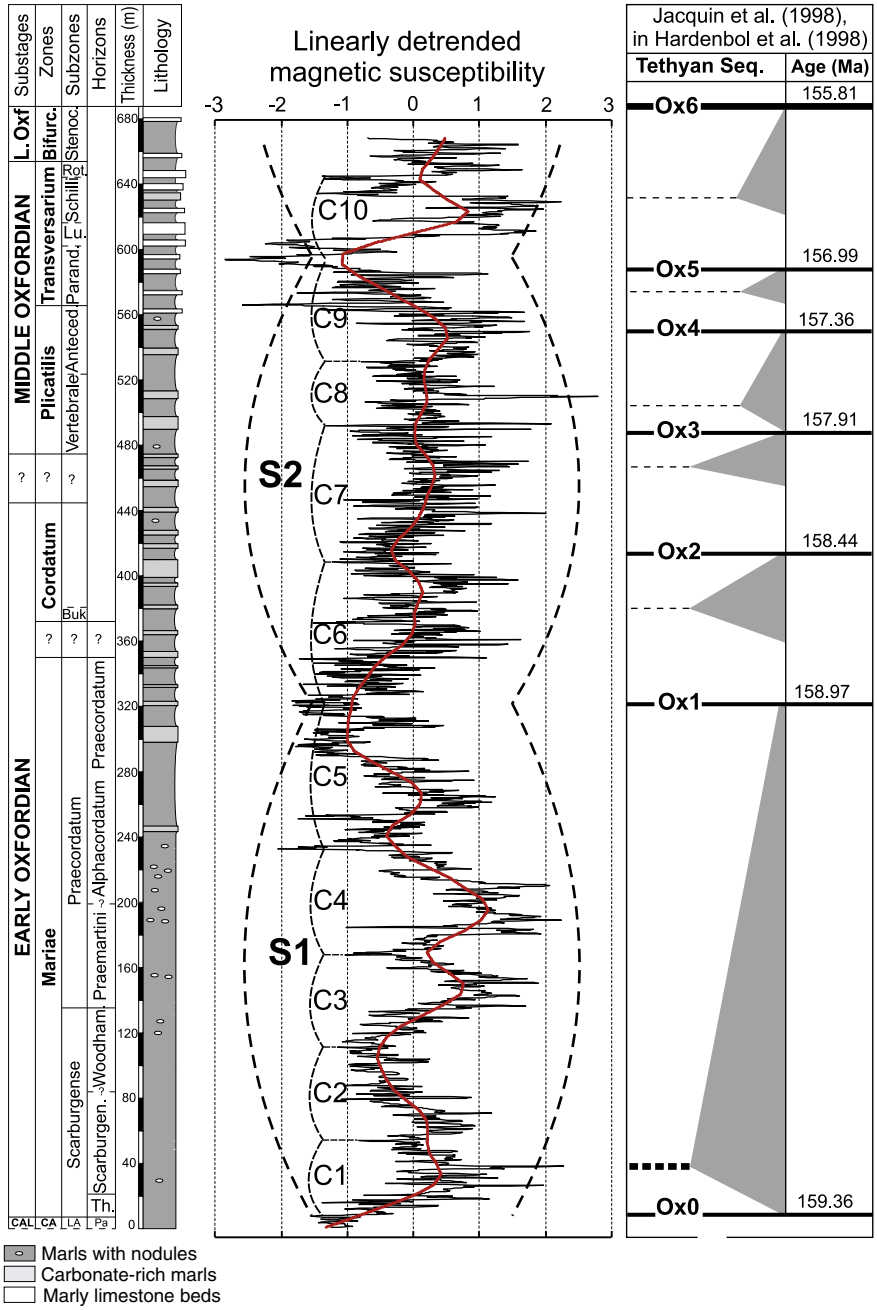

Fig. 9. Comparison of astroclimatic cycles inferred from magnetic susceptibility (MS) variations (Boulila et al., 2010b) with eustatic sequences of the European reference chart (Hardenbol et al., 1998) of early to middle Oxfordian. **(a)** Stratigraphy and high-resolution MS variations of the outcropping Terres Noires Formation (SE France), C1-C10: interpreted 405-kyr eccentricity cycles, S1-S2: interpreted ~2-myr eccentricity cycles (Boulila et al., 2008c, 2010b). **(b)** Eustatic sequence interpretation of Jacquin et al. (1998) (in Hardenbol et al., 1998), Ox0-Ox6: third-order sequence boundaries.

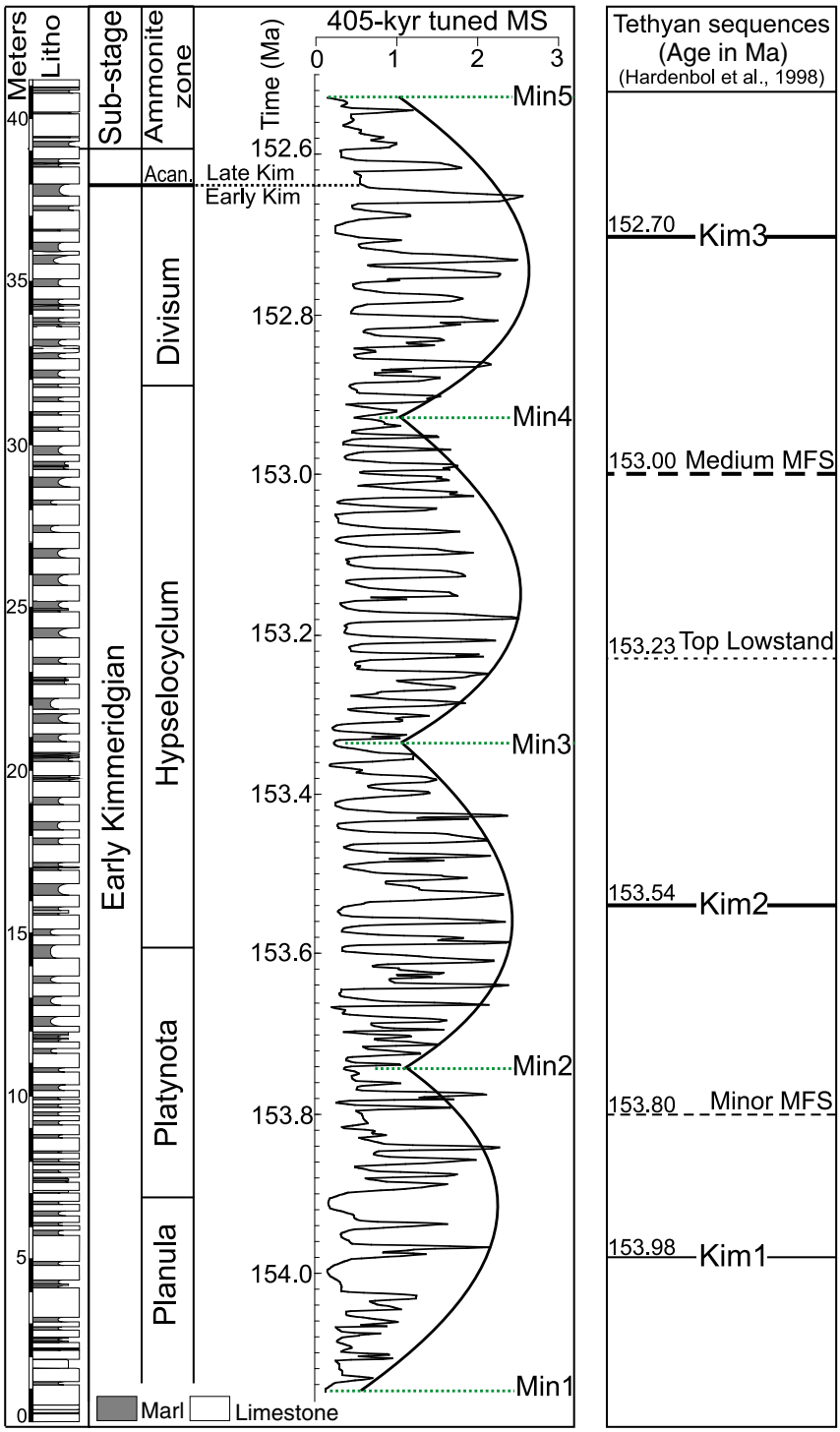

Fig. 10. Comparison of astroclimatic cycles inferred from magnetic susceptibility (MS) variations (Boulila et al., 2008a) with eustatic sequences of the European reference chart (Hardenbol et al., 1998) of early Kimmeridgian (see text for discussion). **(a)** Stratigraphy and high-resolution MS variations of the outcropping La Méouge section (SE France), Min1-Min5: interpreted 405-kyr eccentricity cycles from MS minima, MS minima are interpreted to correspond to maximum flooding surfaces (MFS) (Boulila et al., 2010a, 2011). **(b)** Eustatic sequence interpretation of Jacquin et al. (1998) (in Hardenbol et al., 1998), Kim1-Kim3: third-order sequence boundaries (Jacquin et al., 1998).

Kim1 and Kim3 of the chart was suggested (Boulila et al., 2008b). According to MS cycles, it is placed between Min3 and Min4, i.e. at the top lowstand of Kim2-Kim3 sequence of Hardenbol et al. (1998) (Fig. 10). Our MS time series is too short to cover long-period (~2-myr) eccentricity modulations. However in the Kimmeridge Clay Formation (Dorset, UK), a strong, ~2-myr cyclicity modulating the 405-kyr cycles was detected in physical proxies, and interpreted as drivers of sea-level change (Huang et al., 2010a).

The upper Oxfordian Jura outcrops of Germany, Spain, and Switzerland provide an additional example of astronomical forcing (Fig. 11 ; Strasser et al., 2000). Most sections represent shallow carbonate-dominated platform environments, but deeper-water sections were also studied to allow platform-to-basin correlations (e.g., Strasser et al., 2005). Microfacies analysis highlighted distinct hierarchical stacking patterns and facies evolution, which allowed identification of depositional sequences related to sea-level change. The observed

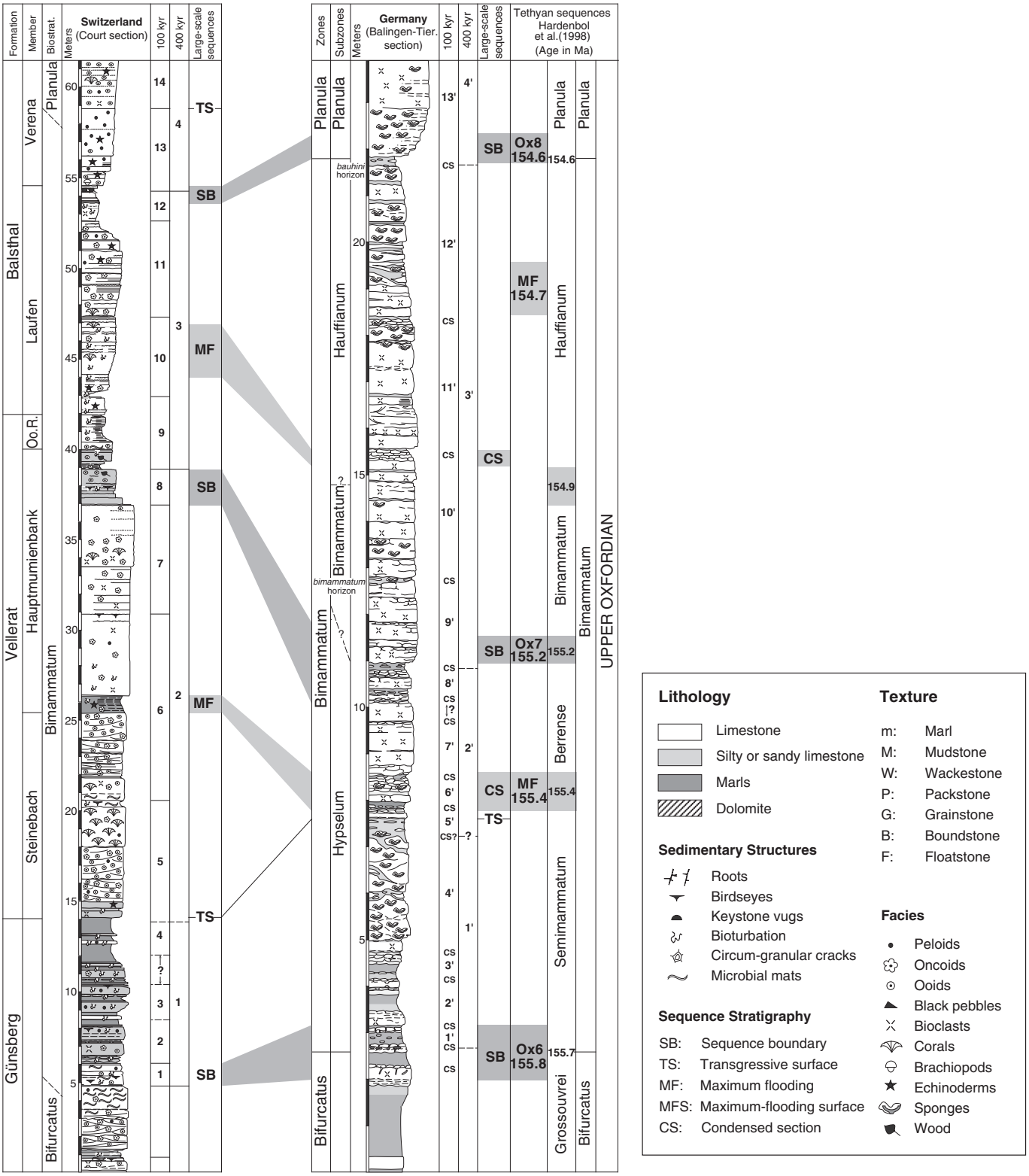

Fig. 11. Correlation between astroclimatic cycles inferred from facies analysis (Strasser et al., 2000) and eustatic sequences of the European reference chart (Jacquin et al., 1998 in Hardenbol et al., 1998) of late Oxfordian (in Strasser et al., 2000). **(a)** Court section (Switzerland). **(b)** Balingen-Tieringen section (Germany). This example among many others of Strasser et al. shows precession/eccentricity control of sea-level depositional sequences during Jurassic greenhouse periods. Here, third-order eustatic sequences are attributed to 405-kyr eccentricity cycles (see text for discussion).

hierarchy of sea-level sequences (elementary, small-scale, and medium-scale sequences) were attributed to orbital frequencies (precession, ~100- and 405-kyr eccentricity, respectively) (Strasser et al., 1999). In particular, the medium-scale (405-kyr) sequences were demonstrated to correspond to third-order sequences of the European eustatic chart of Hardenbol et al. (1998) (Strasser et al., 2000).

These Jurassic sedimentary records suggest that eccentricity-modulation cycles control third-order eustatic sequences. However,

we note that when compared with cyclostratigraphy, third-order sequences of the European eustatic chart (Hardenbol et al., 1998) sometimes match the 405-kyr cycles (Strasser et al., 2000; Boulila et al., 2008a), and sometimes correlate with ~2.4-myr cycles even within the same geological interval (e.g., Oxfordian stage, Boulila et al., 2010b). This confusion highlights the difficulties in deciphering depositional sequences in the absence of a temporal framework for sea-level variations. In this study, we use orbital frequencies to try to provide a temporal hierarchy of eustatic sequences. Constrains from theoretical modelling (Matthews and Frohlich, 2002), and well defined Late Cretaceous sequence stratigraphy (Section 4.1) indicate that the long-period (~2.4-myr) eccentricity cycles correspond to third-order eustatic sequences. Thus, most of the third-order sequences of the European eustatic chart of Hardenbol et al. (1998) may correspond to fourth-order cycles, reflecting the 405-kyr eccentricity cycles (e.g., Strasser et al., 2000; Boulila et al., 2008a, 2010b).

A composite cored section in the Newark basin (eastern North America) represents an almost 5-km thick sequence of lacustrine deposits, spanning a nearly 30-myr interval of the Late Triassic-earliest Jurassic (Olsen and Kent, 1999). Integrated cyclo-magnetostratigraphic studies allowed the recognization of precession and a rich series of eccentricity modulation cycles. In particular, 405-kyr, ~1.75-myr, and ~3.5-myr astroclimatic cycles were detected in sedimentary structures and sediment color proxies (Olsen and Kent, 1999; Olsen, 2001), which correspond respectively to the present 405-kyr, ~2.4-myr, and ~4.6-myr eccentricity cycles (Laskar et al., 2004). These sedimentary cycles reflect lake-level oscillations, which were demonstrated to respond to global climate drivers (Kemp and Coe, 2007). Triassic marine sections also show evidence of precession-eccentricity forcing (e.g., Preto and Hinnov, 2003; Maurer et al., 2004; Gang et al., 2007; Vollmer et al., 2008). Numerous Mesozoic sedimentary records from different depositional environments document the predominance of precession-eccentricity forcing of sea-level change (discussed in part in Fischer et al., 2009). We infer that astroclimatic forcing and the resulting base level variations were mainly connected with significant precession-eccentricity forcing during the Mesozoic greenhouse period.

5. Discussion

5.1. Mechanisms generating sea-level change

A clear relationship between sequence boundaries and glacioeustatic sea-level lowerings has been demonstrated for the "icehouse world" of the past 33.5 Ma and the nascent icehouse world of 33.5-51 Ma (Miller et al., 1998; Pekar et al., 2005). Comparison of the New Jersey-based eustatic estimates with published ice-sheet models and Milankovitch predictions suggests that small (5–10 x 10^6 km^3), ephemeral, and aerially restricted Antarctic ice sheets paced the Late Cretaceous to middle Eocene global sea-level change (Miller et al., 2003, 2005b).

Large (25 to 40 m) and rapid (<1 myr) sea-level drops are known from diverse locations in the Cenomanian, Turonian, and Campanian/Maastrichtian transition of North America (New Jersey), northern Europe, and the Russian Platform (Sahagian et al., 1996; Gale et al., 2002, 2008; Miller et al., 2005b). This demonstrates that these events are global and cannot be ascribed to regional tectonism. Mechanisms for regional tectonism have been invoked to explain sequence boundaries, including: 1) variations in intraplate stress (e.g., Cloetingh, 1988; Karner et al., 1993); 2) density-driven mantle processes related to the interaction of cratons with the subducted slab (e.g., Moucha et al., 2008; Müller et al., 2008), though this mechanism to slow for the myr scale changes discussed here ; and 3) a related mechanism of mantle "hot blobs", areas of vertical motion in the mantle on time scales potentially shorter than 1 myr with amplitudes of tens of meter (Lovell, 2010). We argue that the global nature of major Cenomanian, Turonian, and Campanian/Maastrichtian sequence boundaries excludes these regional tectonic mechanisms.

These greenhouse eustatic oscillations were postulated to be related to the waxing and waning of ephemeral ice sheets in Antarctica (e.g., Miller et al., 2005b). More recent studies by Bornemann et al. (2008) support this idea through evidence of a significant $\delta^{18}O$ increase at ~91.2 Ma in the equatorial Atlantic at Demerara Rise (ODP, Site 1259), which corresponds to Miller et al.'s $\delta^{18}O$ middle Cenomanian (ca. 92–93 Ma) increase. Additionally, Galeotti et al. (2009) found two Cenomanian and Turonian and one Coniacian ice sheet episodes in a study of the bulk carbonate $\delta^{18}O$ record in Italy. Interestingly, they correlated these $\delta^{18}O$ events with well-developed regional sequence boundaries observed on the shallow carbonate platform.

The expression of obliquity modulation frequencies during the Cenozoic "icehouse world" versus eccentricity modulation during the Mesozoic "greenhouse world" may be an indirect indicator of glacioeustatic intensity. Obliquity has a major effect on polar ice sheets, though the poor expression/lack of precessional forcing on ice sheets prior to the last 1 Ma is a mystery that has not been explained (see discussion in Raymo and Huybers, 2008). Thus, during epochs of persistent glaciations (i.e., "icehouse world"), the obliquity signature is strongly expressed in depositional sequences as the major control of the waning and waxing of polar ice sheets (i.e., glacioeustatic control). In contrast, during "greenhouse world" with small ephemeral or no ice sheets, high latitude forcing associated with obliquity may not be the only global mechanism that drives depositional sequences. Precession has been demonstrated as a primary control on greenhouse sea-level oscillations (Section 4). Therefore, obliquity would be less influential, and eccentricity would be the stronger control over sea level and depositional sequences due to its modulation of the precession index (Fig. 10). Intermittent ice sheets were likely present throughout much of the Jurassic to the early Eocene, and could have contributed to sea-level change via a relatively weak glacioeustatic signal (Frakes et al., 1992; Stoll and Schrag, 1996; Miller et al., 1999, 2003, 2005b; Price, 1999; Dromart et al., 2001; Bornemann et al., 2008, Harris et al., 2010). Recent studies have even argued that bipolar icehouse could have existed in Paeocene-Eocene (Tripati et al., 2005, 2008; Eldrett et al., 2007; Spielhagen and Tripati, 2009). During Mesozoic-Cenozoic greenhouse epochs (Triassic to middle Eocene), eustatic change could have been driven by several mechanisms. For example, Milankovitch-scale base-level change during Late Triassic has been attributed to variations in storage of groundwater and lakes. This mechanism could generate at most 5 m of sea-level change (Jacobs and Sahagian, 1993; Sahagian et al., 1996). Likewise, thermal expansion and contraction of seawater column i.e., thermoeustasy could generate only few meters of sea-level oscillation (Gornitz et al., 1992; Schulz and Schäfer-Neth, 1998). Yet, it is clear that the larger events of the Late Cretaceous are far too large to be explained by these mechanisms. Therefore, we speculate that the driver, during the greenhouse, is the eccentricity modulation of precessional forcing of the presence/absence of small continental ice sheets.

5.2. Third-order sequence - eustatic sequence hierarchy

As sea-level change is a major control of depositional sequences via glacioeustasy, thermoeustasy, and/or tectonoeustasy (e.g., Vail et al., 1977, 1991; Haq et al., 1987), the hierarchy of sedimentary sequences were based mainly on amplitude and timing of sea-level oscillations. Eustatic amplitudes could be constrained by isotopic stratigraphy (e.g., $\delta^{18}O$, Miller et al., 1991) or by coupled foraminiferal $\delta^{18}O$ and Mg/Ca (Billups and Schrag, 2002; Lear et al., 2004), and/or sedimentological approaches (e.g., continental onlaps, Vail et al., 1977; backstripping, Kominz and Pekar, 2001). The estimation of sequence durations have often been hampered by several problems

such as sequence identification, sediment preservation, and age models used for sequence duration estimates.

The depositional sequence terminology (hierarchy) that is commonly in use in sedimentology is as follows. First- and second-order sequences are attributed to tectono-eustatic changes (mantle convection and plate tectonics). Fourth, fifth, and sixth orders were linked to climato-eustatic changes driven by Earth's orbital parameters. Third-order sequences were often related to both tectonic and climatic influences (e.g., Vail et al., 1991). Many studies have suggested tectonics as the major driver of third-order sequences (e.g., Cloetingh, 1988; Miall, 1990 ; Karner et al., 1993; Dewey and Pitman, 1998; Lovell, 2010), though these mechanisms fail to explain global sea-level changes. Recent studies have argued that orbitally forced climate is the main control of third-order eustatic sequences via glacioeustasy, thermoeustasy, and/or other processes (Section 5.1).

Even at higher orders, sea-level sequences have been demonstrated to be controlled (so preserved) by precession-eccentricity in Mesozoic greenhouse (e.g., Strasser et al., 1999, 2006) and obliquity in Cenozoic icehouse (e.g., Hays et al., 1976; Zachos et al., 2001a,b ; Huybers and Wunsch, 2005; Naish et al., 2009). The record of orbital cycles in several paleoclimatic proxies and sea-level depositional sequences does not, however, exclude the chaotic behavior of Earth's climate and sedimentary system response to orbital forcing (e.g., Kominz and Pisias, 1979; Huybers, 2009; Meyers and Hinnov, 2010). In this study, we show some evidence of third-order eustatic oscillations in tune with orbital periodicities. Considering this link, we propose a possible view of eustatic sequence hierarchy.

On the basis of orbital frequencies, and assuming that climatic controls played an important role on deposition of third- and higher-order sequences (when preserved) was orbital forcing, we link eustatic hierarchy to orbital frequencies as follows. Third-order sequences may correspond to long-period (~2.4 myr) eccentricity (Mesozoic greenhouse climate), long-period (~1.2 myr) obliquity (Cenozoic icehouse climate) and/or both (transitional climate, earliest Cenozoic). Theoretical modeling studies (Matthews and Frohlich, 2002; DeConto and Pollard, 2003) predicted glacioeustatic falls due to orbital forcing in tune with 405-kyr and ~2.4-myr eccentricity minima. Interestingly, Matthews and Frohlich (2002) predicted glacioeustatic falls that are similar to those obtained from the Late Cretaceous New Jersey margin (Miller et al., 2005b, their Fig. 6). They suggested that the 405-kyr cycles correspond to fourth-order, and the ~2.4-myr cycles to third-order glacioeustatic sequences. Thus, both geological and theoretical data reveal eccentricity forcing of Mesozoic greenhouse sequences.

Long-period orbital modulations in eccentricity and obliquity (i.e., ~2.4- and ~1.2-myr, respectively) are linked through the astronomical resonance between the Earth and Mars (Laskar, 1990). The critical resonant argument (Section 2) is in mode 1:2 (i.e., $(s4-s3)-2(g4-g3)=0$) from the Present to approximately 40 Ma (Laskar et al., 2004, Pälike et al., 2004). Beyond this time, the resonance could cross the 1:1 mode (i.e., $(s4-s3)-(g4-g3)=0$). Thus, the ~2.4- and ~1.2-myr periodicities could significantly vary in deep times. This means that the ~2.4 myr cycle discussed earlier for the Late Cretaceous for e.g. (Fig. 8) and for the Mesozoic in general cannot be predicted (Laskar et al., 2004). Due to resonances, It can deviate to ~1.2 myr and back. This is the same behavior exhibited by the ~1.2 myr cycle beyond 40 Ma, which can switch to ~2.4 myr and back. Olsen and Kent (1999) showed the important control of the long eccentricity cycle on Triassic lake levels, but clearly documented that the periods were closer to 1.75 myr vs. the ~2.4 myr astronomically predicted (Laskar et al., 2004) and that stratigraphically detected (Hilgen et al., 2003) in the Cenozoic. Similarly, the ~1.2 myr tilt cycle is predicatable from astronomical parameters and visible in climate records over the past 40 Ma, but there may be shifts in its true period beyond 40 Ma. Therefore, we use the terms "~2.4 myr" and "~1.2 myr" beyond 40 Ma to simply designate the astronomical origins on the order of 1 and 2 myr periods (i.e., related to g3, g4, s3, and s4), rather than precisely determined periods of the cycles. Accordingly and because of the expression of ~1.2 myr in icehouse sequences and ~2.4 myr in greenhouse sequences, we suggest that these unstable ~1.2- and ~2.4-myr periodicities may be placed within the same eustatic order (i.e., third order).

Stratigraphically well-documented fourth-order sequences (Buonocunto et al., 1999; Grant et al., 1999; Strasser et al., 2000; Gale et al., 2002, 2008; Boulila et al., 2008a, 2010b) could reflect the astronomically stable 405-kyr eccentricity cycle (Laskar et al., 2004) and possibly the ~160- to ~200-kyr short obliquity modulation. Fifth-order sequences would reflect the short (~100-kyr) eccentricity cycle, and finally sixth-order sequences would be linked to the fundamental precession (~20 kyr) and/or obliquity (~40 kyr) cycles. This hierarchy should take into account the evolution of orbital frequencies through geological time. For example, the ~1.2- and ~2.4-myr cycles may have varied beyond the past 40 Ma because of the chaotic motion of the inner planets (Laskar, 1989, 1990; see above). Also, precession and obliquity components were shorter in deep times because of tidal dissipation (Berger et al., 1992; Laskar et al., 2004). Finally, we have to note that this simple link between astronomical and eustatic hierarchies does not rule out several stochastic processes and feedbacks interfering in climate and sea level changes, such as intrinsic ice dynamics, greenhouse gases effects, tectonics, etc.

6. Conclusions

One of the outstanding questions of the past 30 years is the origin (i.e., tectonic or climate) of third-order depositional (eustatic) sequences. Using several Cenozoic and Mesozoic sedimentary records, we note a correspondence between long-period astronomical cycles and third-order sequences hinting at a possible link between the two. At the same time, we do not rule out possible contributions from additional sea-level drivers in our illustrating sedimentary records (e.g., tectonics). Still, most of the third-order sea-level cycles appear to be global, ruling out most of the proposed tectonic mechanisms (e.g., intraplate stress, mantle slab, mantle hot blobs).

Through a correlation between Cenozoic icehouse sequences and astronomical cycles, we demonstrate a close correspondence in number and timing between ~1.2-myr obliquity modulation cycles and third-order sequences, suggesting that there could be a causal link between the two. In contrast, Mesozoic greenhouse sequences seem to be related to ~2.4-myr eccentricity modulation cycles. This differential expression of obliquity in icehouse versus precession-eccentricity in greenhouse worlds may be related to the sensitivity of large polar ice sheets to obliquity forcing. Thus, the major driving process of third-order sequences in an icehouse world is glacioeustasy, while in a greenhouse world, 'weaker' glacioeustasy and/or other climatically driven processes (e.g., thermoeustasy) may have dominated the sea-level record.

Finally, we propose the use of eustatic sequence hierarchy based on the dominant frequencies of orbital controls. Third-order sequences correspond to the astronomically linked ~1.2-myr obliquity and ~2.4-myr eccentricity cycles. The stratigraphically well-recognized fourth-order cycles could be linked to 405-kyr eccentricity and possibly ~160- to ~200-kyr obliquity cycles, fifth-order to ~100-kyr eccentricity, and finally sixth-order to the fundamental obliquity (~40 kyr) and precession (~20 kyr) cycles. This hierarchy should take into account the evolution of orbital frequencies through time. For example, the ~1.2- and ~2.4-myr cycles would vary past to 40 Ma because of the chaotic motion of the inner planets, while, precession and obliquity components decrease in deep times because of the tidal dissipation.

Acknowledgments

S. Boulila, B. Galbrun, and J. Laskar were supported by French ANR Grant ASTS-CM. K.G. Miller was supported by NSF grant OCE0623883.

J. Laskar acknowledges the support from GENCI-CINES and PNP-CNRS. We thank very much Michelle Kominz for help, several significant revisions, advices, and for the time spent with us to considerably ameliorate the manuscript. We are grateful for Editor Paul Wignall. We also thank two anonymous reviewers and Nereo Preto for very helpful reviews that led to important revisions of our manuscript.

References

Al-Husseini, M., 2009. Stratigraphic Note: Update to Late Triassic - Jurassic stratigraphy of Saudi Arabia for the Middle East Geologic Time Scale. GeoArabia 14, 145–186.
Al-Husseini, M., Matthews, R.K., Mattner, J., 2006. Stratigraphic Note: Orbital-forcing calibration of the Late Jurassic (Oxfordian-early Kimmeridgian) Hanifa Formation, Saudi Arabia. GeoArabia 11, 145–149.
Al-Husseini, M.I., Mattews, R.K., 2010. Calibrating Mid-Permian to Early Triassic Khuff sequences with orbital clocks. GeoArabia 15, 171–206.
Anderson, C., Jansen, E., 2003. A Miocene (8–12 Ma) intermediate water benthic stable isotope record from the northeastern Atlantic, ODP site 982. Paleoceanography 18 (1), 1013. doi:10.1029/2001PA000657.
Beaufort, L., 1994. Climatic importance of the modulation of the 100 kyr cycle inferred from 16 m.y. long Miocene records. Paleoceanography 9, 821–834.
Berger, A., Loutre, M.F., Laskar, J., 1992. Stability of the Astronomical Frequencies Over the Earth's History for Paleoclimate Studies. Science 255, 560–566.
Billups, K., Schrag, D.P., 2002. Paleotemperatures and ice volume of the past 27 Myr revisited with paired Mg/Ca and 18O/16O measurements on benthic foraminifera. Paleoceanography 17 (1), 1003. doi:10.1029/2000PA000567.
Billups, K., Channell, J.E.T., Zachos, J.C., 2002. Late Oligocene to early Miocene geochronology and paleoceanography from the subantarctic South Atlantic. Paleoceanography 17 (1004). doi:10.1029/2000PA000568.
Bornemann, A., Norris, R.D., Friedrich, O., Beckmann, B., Schouten, S., Sinninghe Damsté, J.S., Vogel, J., Hofmann, P., Wagner, T., 2008. Isotopic evidence for glaciation during the Cretaceous supergreenhouse. Science 319, 189–192.
Boulila, S., 2008. Cyclostratigraphie des séries sédimentaires du Jurassique supérieur (Sud-Est de la France, Nord de la Tunisie): contrôle astro-climatique, implications géochronologiques et séquentielles. Ph.D. Thesis, Pierre et Marie Curie University, Paris, France. p. 313.
Boulila, S., Galbrun, B., Hinnov, L.A., Collin, P.Y., 2008a. Orbital calibration of the Early Kimmeridgian (southeastern France): implications for geochronology and sequence stratigraphy. Terra Nova 20, 455–462.
Boulila, S., Galbrun, B., Hinnov, L.A., Collin, P.Y., 2008b. High-resolution cyclostratigraphic analysis from magnetic susceptibility in a Lower Kimmeridgian (Upper Jurassic) marl-limestone succession (La Méouge, Vocontian Basin, France). Sedimentary Geology 203, 54–63.
Boulila, S., Hinnov, L.A., Huret, E., Collin, P.Y., Galbrun, B., Fortwengler, D., Marchand, D., Thierry, J., 2008c. Astronomical calibration of the Early Oxfordian (Vocontian and Paris basins, France): consequences of revising the Late Jurassic time scale. Earth and Planetary Science Letters 276, 40–51.
Boulila, S., de Rafélis, M., Hinnov, L.A., Gardin, S., Galbrun, B., Collin, P.Y., 2010a. Orbitally forced climate and sea-level changes in the Paleoceanic Tethyan domain (marl-limestone alternations, Lower Kimmeridgian, SE France). Palaeogeography Palaeoclimatology Palaeoecology 292, 57–70.
Boulila, S., Galbrun, B., Hinnov, L.A., Collin, P.Y., Ogg, J.G., Fortwengler, D., Marchand, D., 2010b. Milankovitch and sub-Milankovitch forcing of the Oxfordian (Late Jurassic) Terres Noires Formation (SE France) and global implications. Basin Research 22, 717–732.
Boulila, S., Gardin, S., de Rafélis, M., Hinnov, L.A., Galbrun, B., Collin, P.Y., 2011. Reply to the Comment on "Orbitally forced climate and sea-level changes in the Paleoceanic Tethyan domain (marl-limestone alternations, Lower Kimmeridgian, SE France)" by S. Boulila et al. (2010a). Palaeogeography Palaeoclimatology Palaeoecology 306, 252–257.
Browning, J.V., Miller, K.G., Pak, D.K., 1996. Global implications of Eocene greenhouse and doubthouse sequences on the New Jersey coastal plain: the icehouse cometh. Geology 24, 639–642.
Browning, J.V., Miller, K.G., Sugarman, P.J., Kominz, M.A., McLaughlin, P.P., Kulpecz, A.A., Feigenson, M.D., 2008. 100 Myr record of sequences, sedimentary facies and sea level change from Ocean Drilling Program onshore coreholes, US Mid-Atlantic coastal plain. Basin Research 20, 227–248.
Buonocunto, F.P., D'Argenio, B., Ferreri, V., Sandulli, R., 1999. Orbital cyclostratigraphy and sequence stratigraphy of Upper Cretaceous platform carbonates at Monte Sant'Erasmo, southern Apennines, Italy. Cretaceous Research 20, 81–95.
Christie-Blick, N., Mountain, G.S., Miller, K.G., 1990. Seismic stratigraphic record of sea-level change. Sea-Level Change, National Academy of Sciences Studies in Geophysics. National Academy Press, Washington, D.C, pp. 116–140.
Cloetingh, S., 1988. Intraplate stresses: a tectonic cause for third-order cycles in apparent sea level? Society of Economic Paleontologists and Mineralogists Special Publication 42, 19–29.
De Verteuil, L., 1997. Palynological delineation and regional correlation of lower Oligiocene through upper Miocene sequences in the Cape Bay and Atlantic City boreholes, New Jersey coastal plain. Proc. Ocean Drill. Program, Sci. Results, 150X, pp. 129–145.
DeConto, R.M., Pollard, D., 2003. Rapid Cenozoic glaciation of Antarctica induced by declining atmospheric CO2. Nature 421, 245–249.
Dewey, J.F., Pitman, W.C., 1998. Seal-level changes: Mechanisms, magnitudes and rates. In: Pindell, J.L., Drake, C.L. (Eds.), Paleogeographic evolution and non-glacial eustasy, northern South America: SEPM (Soc. Sed. Geol.), Spec. Publ., 58, pp. 1–17.
Dromart, G., Garcia, J.P., Picard, S., Rousseau, M., Atrops, F., Lécuyer, C., Sheppard, S.M.F., 2001. Perturbation of the carbon cycle at the Middle/Late Jurassic transition: geological and geochemical evidence. American Journal of Science 303, 667–707.
Eldrett, J.S., Harding, I.C., Wilson, P.A., Butler, E., Roberts, A.P., 2007. Continental ice in Greenland during the Eocene and Oligocene. Nature 446 (7132), 176–179.
Fischer, A.G., 1986. Climatic rhythms recorded in strata. Annual Review of Earth and Planetary Sciences 14, 351–376.
Fischer, A.G., Hilgen, F.J., Garrison, R.E., 2009. Mediterranean contributions to cyclostratigraphy and astrochronology. Sedimentology 56, 63–94.
Frakes, L.A., Francis, J.E., Syktus, J.I., 1992. Climate Modes of the Phanerozoic: the History of the Earth's Climate over the past 600 Million Years. Cambridge University Press, Cambridge, p. 274.
Gale, A.S., Hardenbol, J., Hathway, B., Kennedy, W.J., Young, J.R., Phansalkar, V., 2002. Global correlation of Cenomanian (Upper Cretaceous) sequences: Evidence for Milankovitch control on sea level. Geology 30, 291–294.
Gale, A.S., Voigt, S., Sageman, B.B., Kennedy, W.J., 2008. Eustatic sea-level record for the Cenomanian (Late Cretaceous) – Extension to the Western Interior Basin, USA. Geology 36, 859–862.
Galeotti, S., Rusciadelli, G., Sprovieri, M., Lanci, L., Gaudio, A., Pekar, S., 2009. Sea-level control on facies architecture in the Cenomanian–Coniacian Apulian margin (Western Tethys): A record of glacio-eustatic fluctuations during the Cretaceous greenhouse? Palaeogeography Palaeoclimatology Palaeoecology 276, 196–205.
Gang, G., JinNan, T., ShiHong, Z., Jie, Z., LingYan, B., 2007. Cyclostratigraphy of the Induan (Early Triassic) in West Pingdingshan Section, Chaohu, Anhui Province. Science in China Series D Earth Sciences 22–29. doi:10.1007/s11430-007-0156-z.
Ghil, M., Allen, R.M., Dettinger, M.D., Ide, K., Kondrashov, D., Mann, M.E., Robertson, A., Saunders, A., Tian, Y., Varadi, F., Yiou, P., 2002. Advanced spectral methods for climatic time series. Reviews of Geophysics 40 (1) 3.1–3.41.
Gornitz, V., Lebedeff, S., Hansen, J., 1992. Global sea-level trend in the past century. Science 215, 1611–1614.
Gradstein, F.M., Ogg, J.G., Smith, A.G., 2004. A Geologic Time Scale 2004, Cambridge University Press. , p. 589.
Grant, S.F., Coe, A.L., Armstrong, H.A., 1999. Sequence stratigraphy of the Coniacian succession of the Anglo-Paris Basin. Geological Magazine 136, 17–38.
Haq, U.B., Hardenbol, J., Vail, P.R., 1987. Chronology of fluctuating sea levels since the Triassic. Science 235, 1156–1167.
Hardenbol, J., Thierry, J., Farley, M.B., Jacquin, T., Graciansky, P.C., de Vail, P.R., 1998. Mezozoic and Cenozoic sequence chronostratigraphic framework of European basins. SEPM, Spec. Publ., 60, p. 60. Tulsa, OK, 8 charts.
Harris, A., Miller, K.G., Browning, J.V., Sugarman, P.J., Olsson, R.K., Cramer, B.S., Wright, J.D., 2010. ntegrated Stratigraphic Studies of Paleocene-Lowermost Eocene Strata, New Jersey Coastal Plain: Evidence for glacioeustatic control. Paleoceanography. doi:10.1029/2009PA001800.
Hays, J.D., Imbrie, J., Schackleton, N.J., 1976. Variations in the Earth's orbit: Pacemaker of the ice ages. Science 194, 1121–1132.
Hilgen, F.J., Abdul Aziz, H., Krijgsman, W., Raffi, I., Turco, E., 2003. Integrated stratigraphy and astronomical tuning of the Serravallian and lower Tortonian at Monte dei Corvi (Middle-Upper Miocene, northern Italy). Palaeogeography Palaeoclimatology Palaeoecology 199, 229–264.
Hinnov, L.A., 2000. New perspectives on orbitally forced stratigraphy. Annual Review of Earth and Planetary Sciences 28, 419–475.
Hinnov, L.A., Ogg, J.G., 2007. Cyclostratigraphy and the astronomical time scale. Stratigraphy 4, 239–251.
Holbourn, A., Kuhnt, W., Schulz, M., Flores, J.-A., Andersen, N., 2007. Orbitally-paced climate evolution during the middle Miocene "Monterey" carbon-isotope excursion. Earth and Planetary Science Letters 261, 534–550.
Huang, C., Hesselbo, S.P., Hinnov, L.A., 2010a. Astrochronology of the late Jurassic Kimmeridge Clay (Dorset, England) and implications for Earth system processes. Earth and Planetary Science Letters 289, 242–255.
Huang, C., Hinnov, L.A., Fischer, A.G., Grippo, A., Herbert, T., 2010b. Astronomical tuning of the Aptian Stage from Italian reference sections. Geology 38, 899–902.
Huybers, P., 2009. Pleistocene glacial variability as a chaotic response to obliquity forcing. Climate of the Past 5, 481–488.
Huybers, P., Denton, G., 2008. Antarctic temperature at orbital time scales controlled by local summer duration. Nature Geoscience 1, 787–792.
Huybers, P., Wunsch, C., 2005. Obliquity pacing of the late Pleistocene glacial terminations. Nature 434, 491–494.
Imbrie, J., Hays, J.D., Martinson, D.G., McIntyre, A., Mix, A.C., Morely, J.J., Pisias, N.G., Prell, W.L., Shackleton, N.G., 1984. The orbital theory of Pleistocene climate : support from a revised chronology of the marine δ^{18}O record. In: Berger, A.L., Imbrie, J., Hays, J.D., Kukla, G., Saltzman, B. (Eds.), Milankovitch and Climate, Part 1. D. Reidel Publishing Co., Dordrecht, pp. 269–305.
Jacobs, D.K., Sahagian, D.L., 1993. Climate-induced fluctuations in sea level during non-glacial times. Nature 361, 710–712.
Jacquin, T., Dardeau, G., Durlet, C., de Graciansky, P.C., Hantzpergue, P., 1998. The North Sea cycle : An overview of 2nd order transgressive/regressive facies cycles in Western Europe. SEPM Special Publication 60, 445–446.
John, C.M., Karner, G.D., Mutti, M., 2004. δ^{18}O and Marion Plateau backstripping: Combining two approaches to constrain late middle Miocene eustatic amplitude. Geology 32, 829–832.
John, C.M., Karner, G.D., Browning, E., Leckie, R.M., Mateo, Z., Carson, B., Lowery, C., 2011. Timing and magnitude of Miocene eustasy derived from the mixed siliciclastic carbonate stratigraphic record of the northeastern Australian margin. Earth and Planetary Science Letters 304, 455–467.
Karner, G.D., Driscoll, N.W., Weissel, J.K., 1993. Response of the lithosphere to in-plane force variations. Earth and Planetary Science Letters 114, 397–416.

Kemp, D.B., Coe, A.L., 2007. A nonmarine record of eccentricity forcing through the Upper Triassic of southwest England and its correlation with the Newark Basin astronomically calibrated geomagnetic polarity time scale from North America. Geology 35, 991–994.
Kominz, M.A., Pekar, S.F., 2001. Oligocene eustasy from two-dimentional sequence stratigraphic backstripping. Geological Society of America Bulletin 113, 291–304.
Kominz, M.A., Pisias, N.G., 1979. Pleistocene climate: deterministic or stochastic? Science 204, 171–173.
Kominz, M.A., Miller, K.G., Browning, J.V., 1998. Long-term and short-term global sea-level estimates. Geology 26, 311–314.
Kominz, M.A., Browning, J.V., Miller, K.G., Sugarman, P.J., Minzintseva, S., Scotese, C.R., 2008. Late Cretaceous to Miocene sea-level estimates from the New Jersey and Delaware plain coreholes: an error analysis. Basin Research 20, 211–226.
Laskar, J., 1989. A numerical experiment on the chaotic behaviour of the Solar System. Nature 338, 237–238.
Laskar, J., 1990. The chaotic motion of the Solar System: A numerical estimate of the size of the chaotic zone. Icarus 88, 266–291.
Laskar, J., 1999. The limits of the Earth orbital calculations for geological time-scale use. Philosophical Transactions of the Royal Society of London Series A 357, 1735–1759.
Laskar, J., Joutel, F., Boudin, F., 1993. Orbital, precessional, and insolation quantities for the Earth from −20 Myr to +10 Myr. Astronomy and Astrophysics 270, 522–533.
Laskar, J., Robutel, P., Joutel, F., Gastineau, M., Correia, A.C.M., Levrard, B., 2004. A long-term numerical solution for the insolation quantities of the Earth. Astronomy and Astrophysics 428, 261–285.
Laskar, J., Fienga, A., Gastineau, M., Manche, H., 2011. La2010: a new orbital solution for the long term motion of the Earth. Astronomy and Astrophysics 532, A89. doi: 10.1051/0004-6361/201116836.
Lear, C.H., Rosenthal, Y., Coxall, H.K., Wilson, P.A., 2004. Late Eocene to early Miocene ice sheet dynamics and the global carbon cycle. Paleoceanography 19, PA4015. doi:10.1029/2004PA001039.
Lirer, F., Harzhauser, M., Pelosi, N., Piller, W.E., Schmid, H.P., Sprovieri, M., 2009. Astronomically forced teleconnection between Paratethyan and Mediterranean sediments during the Middle and Late Miocene. Palaeogeography Palaeoclimatology Palaeoecology 275, 1–13.
Lourens, L.J., Hilgen, F.J., 1997. Long-periodic variations in the earth's obliquity and their relation to third-order eustatic cycles and Late Neogene glaciations. Quaternary International 40, 43–52.
Lovell, B., 2010. A pulse in the planet : regional control of high-frequency changes in relative sea level by mantle convection. Journal of the Geological Society of London 167, 637–648.
Mattews, R.K., Al-Husseini, M.I., 2010. Orbital-forcing glacio-eustasy: A sequence stratigraphic time scale. GeoArabia 15, 129–142.
Matthews, R.K., Frohlich, C., 2002. Maximum flooding surfaces and sequence boundaries: comparisons between observations and orbital forcing in the Cretaceous and Jurassic (65–190 Ma). GeoArabia 7, 503–538.
Maurer, F., Hinnov, L.A., Schlager, W., 2004. Statistical time-series analysis and sedimentological tuning of bedding rhythms in a Triassic basinal succession (Southern Alps, Italy). In: D'Argenio, B., Fischer, A.G., Premoli Silva, I., Weissert, H., Ferreri, V. (Eds.), Cyclostratigraphy: Approaches and Case Histories: SEPM, Spec. Publ., 81, pp. 83–99.
Meyers, S.R., Hinnov, L.A., 2010. Northern Hemisphere glaciation and the evolution of Plio-Pleistocene climate noise. Paleoceanography 25, PA3207. doi:10.1029/2009PA001834.
Miall, A.D., 1990. Principles of Sedimentary Basin Analysis2nd edition. Springer, Berlin.
Miller, K.G., Mountain, G.S., 1996. Drilling and Dating New Jersey Oligocene-Miocene Sequences: Ice Volume, Global Sea Level, and Exxon Records. Science 271, 1092–1095.
Miller, K.G., Wright, J.D., Fairkanks, R.G., 1991. Unlocking the ice house: Oligocene-Miocene oxygen isotopes, eustasy, and margin erosion. Journal of Geophysical Research 96, 6829–6848.
Miller, K.G., Mountain, G.S., Browning, J.V., Kominz, M.A., Sugarman, P.J., Christie-Blick, N., Katz, M.E., Wright, J.D., 1998. Cenozoic global sea level, sequences, and the New Jersey Transect: Results from coastal plain and continental slope drilling. Reviews of Geophysics 36, 569–601.
Miller, K.G., Barrera, E., Olsson, R.K., Sugarman, P.J., Savin, S.M., 1999. Does ice drive early Maastrichtian eustasy? Global $\delta^{18}O$ and New Jersey sequences. Geology 27, 783–786.
Miller, K.G., Sugarman, P.J., Browning, J.V., Kominz, M.A., Hernandez, J.C., Olsson, R.K., Wright, J.D., Feigenson, M.D., Van Sickel, W., 2003. A chronology of Late Cretaceous sequences and sea-level history: glacioeustasy during the Greenhoouse World. Geology 31, 585–588.
Miller, K.G., Sugarman, P.J., Browning, J.V., Kominz, M.A., Olsson, R.K., Feigenson, M.D., Hernandez, J.C., 2004. Upper Cretaceous sequences and sea-level history, New Jersey Coastal Plain. Geological Society of America Bulletin 116, 368–393.
Miller, K.G., Kominz, M.A., Browning, J.V., Wright, J.D., Mountain, G.S., Katz, M.E., Sugarman, P.J., Cramer, B.S., Christie-Blick, N., Pekar, S.F., 2005a. The Phanerozoic record of global sea-level change. Science 310, 1293–1298.
Miller, K.G., Wright, J.D., Browning, J.V., 2005b. Visions of ice sheets in a greenhouse world. Marine Geology 217, 215–231.
Miller, K.G., Browning, J.V., Aubry, M.P., Wade, B.S., Katz, M.E., Kulpecz, A.A., Wright, J., 2008. Eocene-Oligocene global climate and sea-level changes: St. Stephens Quarry, Alabama. Geological Society of America Bulletin 120, 34–53.
Miller, K.G., Mountain, G.S., Wright, J.D., Browning, 2011. A 180-million-year record of sea level and ice volume variations from continental margin and deep-sea isotopic records. Oceanography 24 (2), 40–53.
Mitchell, R.N., Bice, D.M., Montanari, A., Cleavel, L.C., Christianson, K.T., Coccioni, R., Hinnov, L.A., 2008. Oceanic Anoxic Cycles? Orbital prelude to the Bonarelli Level (OAE 2). Earth and Planetary Science Letters 267, 1–16.
Mizintseva, S.F., Browning, J.V., Miller, K.G., 2009. Integrated late Santonian-early Campanian sequence stratigraphy, New Jersey coastal plain: Implications to global sea-level studies. Stratigraphy 6, 45–60.
Moucha, R., Forte, A.M., Mitrovica, J.X., Rowley, D.B., Quere, S., Simmons, N.A., Grand, S.P., 2008. Dynamic topography and long-term sea-level variations: There is no such thing as a stable continental platform. Earth and Planetary Science Letters 271, 101–108.
Müller, R.D., Sdrolias, M., Gaina, C., Steinberger, B., Heine, C., 2008. Long-term sea-level fluctuations driven by ocean basin dynamics. Science 319, 1357–1362.
Naish, et al., 2009. Obliquity-paced Pliocene West Antarctic ice sheet oscillations. Nature 458, 322–329.
Olsen, P.E., 2001. Grand cycles of the Milankovitch band. Eos Transactions of the American Geophysical Union 47 (Supplement 82), F2 Abstract U11A-11.
Olsen, P.E., Kent, D.V., 1999. Long-term Milankovitch cycles from the Late Triassic and Early Jurassic of eastern North America and their implications for the calibration of the Early Mesozoic timescale and the long term behavior of the planets. Philosophical Transactions of the Royal Society of London Series A 357, 1761–1788.
Pälike, H., Laskar, J., Shackleton, N.J., 2004. Geologic constraints on the chaotic diffusion of the Solar System. Geology 32, 929–932.
Pälike, H., Frazier, J., Zachos, J.C., 2006a. Extended orbitally forced palaeoclimatic records from the equatorial Atlantic Ceara Rise. Quaternary Science Reviews 25, 3138–3149.
Pälike, H., Norris, R.D., Herrle, J.O., Wilson, P.A., Coxall, H.K., Lear, C.H., Shackleton, N.J., Tripati, A.K., Wade, B.S., 2006b. The Heartbeat of the Oligocene Climate System. Science 314, 1894–1898.
Pekar, S.F., DeConto, R.M., 2006. High-resolution ice-volume estimates for the early Miocene: Evidence for a dynamic ice sheet in Antarctica. Palaeogeography Palaeoclimatology Palaeoecology 231, 101–109.
Pekar, S.F., Kominz, M.A., 2001. Two-dimentional paleoslope modeling: A new method for estimating water depths for benthic foraminiferal biofacies and paleo shelf margins. Journal of Sedimentary Research 71, 608–620.
Pekar, S.F., Miller, K.G., 1996. New Jersey Oligocene "Icehouse" sequences (ODP Leg 150X) correlated with global $\delta^{18}O$ and Exxon eustatic records. Geology 24, 567–570.
Pekar, S.F., Miller, K.G., Kominz, M.A., 2000. Reconstructing the stratal geometry of latest Eocene to Oligocene sequences in New Jersey: resolving a patchwork distribution into a clear pattern of progradation. Sedimentary Geology 134, 93–109.
Pekar, S.F., Christie-Blick, N., Kominz, M.A., Miller, K.G., 2001. Evaluating the stratigraphic response to eustasy from Oligocene strata in New Jersey. Geology 29, 55–58.
Pekar, S.F., Christie-Blick, N., Kominz, M.A., Miller, K.G., 2002. Calibrating eustasy to oxygen isotopes for the early icehouse world of the Oligocene. Geology 30, 903–906.
Pekar, S.F., Hucks, A., Fuller, M., Li, S., 2005. Glacioeustatic changes in the early and middle Eocene (51–42 Ma): Shallow-water stratigraphy from ODP Leg 189 Site 1171 (South Tasman Rise) and deep-sea $\delta^{18}O$ records. Geological Society of America Bulletin 117, 1081–1093.
Preto, N., Hinnov, L.A., 2003. Unraveling the origin of carbonate platform cyclotherms in the upper Triassic Dürrenstein Formation (Dolomites, Italy). Journal of Sedimentary Research 73, 774–789.
Price, E.D., 1999. The evidence and implications of polar ice during the Mesozoic. Earth-Science Reviews 48, 183–210.
Raymo, M.E., Huybers, P., 2008. Unlocking the mysteries of the ice ages. Nature 451, 284–285.
Sahagian, D., Pinous, O., Olferiev, A., Zakaharov, V., Beisel, A., 1996. Eustatic curve for middle Jurassic-Cretaceous based on Russian platform and Siberian stratigraphy: Zonal resolution. The American Association of Petroleum Geologists Bulletin 80, 1433–1458.
Schulz, M., Schäfer-Neth, C., 1998. Translating Milankovitch climate forcing into eustatic fluctuations via thermal deep water expansion: a conceptual link. Terra Nova 9, 228–231.
Shackleton, N.J., Hall, M.A., 1997. The late Miocene stable isotope record, site 926. In: Shackleton, N.J., Curry, W.B., Richter, C., Bralower, T.J. (Eds.), Proc. ODP, Sci. Results, vol. 154. Ocean Drilling Program, College Station, TX, pp. 367–373.
Shackleton, N.J., Crowhurst, S.J., Weedon, G.P., Laskar, J., 1999. Astronomical calibration of Oligocene-Miocene time. Philosophical Transactions of the Royal Society of London Series A 357, 1907–1929.
Sloss, L.L., 1963. Sequences in the cratonic interior of North America. Geological Society of America Bulletin 74, 93–114.
Spielhagen, R.F., Tripati, A., 2009. Evidence from Svalbard for near-freezing temperatures and climate oscillations in the Arctic during the Paleocene and Eocene. Palaeogeography Palaeoclimatology Palaeoecology 278, 48–56.
Stoll, H.M., Schrag, D.P., 1996. Evidence for glacial control of rapid sea level changes in the early Cretaceous. Science 272, 1771–1774.
Strasser, A., Pittet, B., Hillgärtner, H., Pasquier, J.B., 1999. Depositional sequences in shallow carbonate-dominated sedimentary systems: concepts for a high-resolution analysis. Sedimentary Geology 128, 201–221.
Strasser, A., Hillgärtner, H., Hug, W., Pittet, B., 2000. Third-order depositional sequences reflecting Milankovitch cyclicity. Terra Nova 12, 303–311.
Strasser, A., Aurell, M., Bádenas, B., Meléndez, G., Tomás, S., 2005. From platform to basin to swell: orbital control on sedimentary sequences in the Oxfordian, Spain. Terra Nova 17, 407–413.
Strasser, et al., 2006. Cyclostratigraphy – concepts, definitions, and applications. Newsletters on Stratigraphy 42 (2), 75–114.
Sugarman, P.J., Miller, K.G., Browning, J.V., Kulpecz, A.A., McLaughlin, P.P., Monteverde, D.H., 2005. Hydrostratigraphy of the New Jersey Coastal Plain: Sequences and facies predict continuity of aquifers and confining units. Stratigraphy 2, 259–276.

Taner, M.T., 2000. Attributes Revisited, Technical Publication. Rock Solid Images, Inc., Houston, Texas. URL: http://www.rocksolidimages.com/pdf/attrib_revisited.htm.
Tripati, A.K., Backman, J., Elderfield, J., Perretti, P., 2005. Eocene bipolar glaciation associated with global carbon cycle changes. Nature 436 (7049), 341–346.
Tripati, A.K., Eagle, R.A., Morton, A., Dowdeswell, J.A., Atkinson, K.L., Bahe, Y., Dawber, C.F., Khadun, E., Shaw, R.M.H., Shorttle, O., Thanabalasundaram, L., 2008. Evidence for Northern Hemisphere glaciation back to 44 Ma from ice-rafted debris in the Greenland Sea. Earth and Planetary Science Letters 256 (1–2), 112–122.
Turco, E., Bambini, A.M., Foresi, L., Iaccarino, S., Lirer, F., Mazzei, R., Salvatorini, G., 2002. Middle Miocene high-resolution calcareous plankton biostratigraphy at Site 926 (Leg 154, equatorial Atlantic Ocean): palaeoecological and palaeobiological implications. Geobios 35, 257–276 (mémoire spécial no. 24).
Vail, P.R., Mitchum, R.M., Todd, J.R.G., Widmier, J.M., Thompson, S., Sangree, J.B., Bubb, J.N., Hatlelid, W.G., 1977. In: Payton, C.E. (Ed.), Seismic stratigraphy and global changes of sea level: Seismic Stratigraphy – Applications to Hydrocarbon Exploration. Mem. Am. Ass. Pertol. Geol., 26, pp. 49–212.
Vail, P.R., Audemard, F., Bowman, S.A., Eisner, P.N., Perez-Cruz, C., 1991. The stratigraphic signatures of tectonics, eustasy and sedimentology – an overview. In: Einsele, G., et al. (Ed.), Cycles and Events in Stratigraphy. Springer, Berlin, pp. 617–659.
Van Sickel, W.A., Kominz, M.A., Miller, K.G., Browning, J.V., 2004. Late Cretaceous and Cenozoic sea-level estimates: backstripping analysis of borhole data, onshore New Jersey. Basin Research 16, 451–465.
Vollmer, T., Werner, R., Weber, M., Tougiannidis, N., Röhling, H.G., Hambach, U., 2008. Orbital control on Upper Triassic Playa cycles of the Steinmergel-Keuper (Norian): A new concept for ancient playa cycles. Palaeogeography Palaeoclimatology Palaeoecology 267, 1–16.
Wade, B.S., Pälike, H., 2004. Oligocene climate dynamics. Paleoceanography 19, PA4019. doi:10.1029/2004PA001042.
Westerhold, T., Bickert, T., Röhl, U., 2005. Middle to late Miocene oxygen isotope stratigraphy of ODP site 1085 (SE Atlantic): new constraints on Miocene climate variability and sea-level fluctuations. Palaeogeography Palaeoclimatology Palaeoecology 217, 205–222.
Zachos, J.C., Pagani, M., Sloan, L., Thomas, E., Billups, K., 2001a. Trends, Rhythms, and Aberrations in Global Climate 65 Ma to Present. Science 292, 686–693.
Zachos, J.C., Shackleton, N.J., Revenaugh, J.S., Pälike, H., Flower, B.P., 2001b. Climate response to orbital forcing across the Oligocene-Miocene boundary. Science 292, 274–278.